

RD-A186 445

THE SYNTHESIS AND CHARACTERIZATION OF SOME RARE EARTH
ARSENIDES(U) AEROSPACE CORP EL SEGUNDO CA MATERIALS
SCIENCES LAB J N SCHURR 10 SEP 87 TR-0006(6935-87)-1

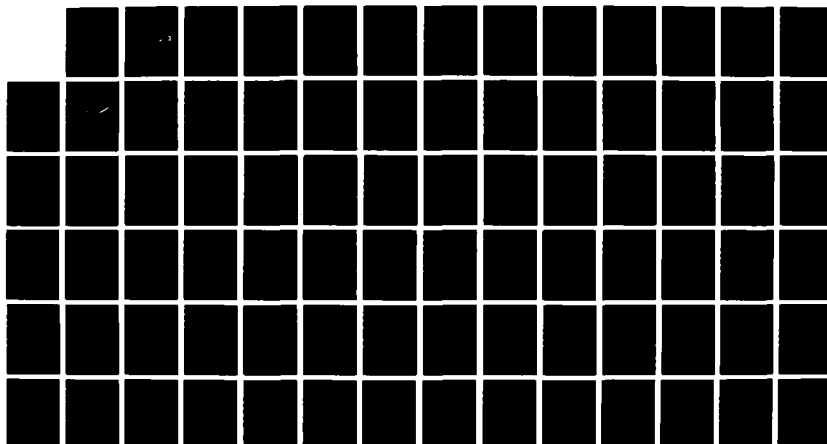
1/1

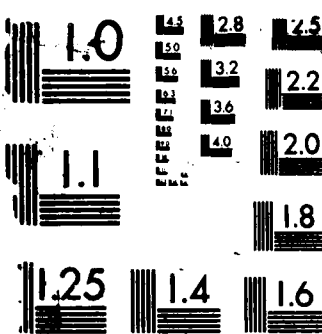
UNCLASSIFIED

SD-TR-87-40 F04701-85-C-0006

F/G 7/2

NL





MICROCOPY RESOLUTION TEST CHART
NATIONAL BUREAU OF STANDARDS-1963-A

FILE COPY

REPORT SD-TR-87-40

12

AD-A186 445

The Synthesis and Characterization of Some Rare Earth Arsenides

J. N. SCHURR
Materials Sciences Laboratory
Laboratory Operations
The Aerospace Corporation
El Segundo, CA 90245-4691

10 September 1987

DTIC
SELECTED
S D
OCT 22 1987
8 D

Prepared for
SPACE DIVISION
AIR FORCE SYSTEMS COMMAND
Los Angeles Air Force Station
P.O. Box 92960, Worldway Postal Center
Los Angeles, CA 90009-2960

APPROVED FOR PUBLIC RELEASE;
DISTRIBUTION UNLIMITED

071015 115

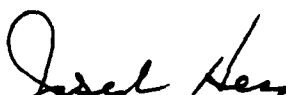
This report was submitted by The Aerospace Corporation, El Segundo, CA 90245, under Contract No. F04701-85-C-0086 with the Space Division, P.O. Box 92960, Worldway Postal Center, Los Angeles, CA 90009-2960. It was reviewed and approved for The Aerospace Corporation by R. W. Fillers, Director, Materials Sciences Laboratory. Captain Annetta Weber, SD/CNIV, was the project officer for the Mission-Oriented Investigation and Experimentation (MOIE) program.

This report has been reviewed by the Public Affairs Office (PAS) and is releasable to the National Technical Information Service (NTIS). At NTIS, it will be available to the general public, including foreign nationals.

This technical report has been reviewed and is approved for publication. Publication of this report does not constitute Air Force approval of the report's findings or conclusions. It is published only for the exchange and stimulation of ideas.



ANNETTA WEBER, Capt, USAF
MOIE Project Officer
SD/CNIV



JOSEPH HESS, GM-15
Director, AFSTC West Coast Office
AFSTC/WCO OL-AB

UNCLASSIFIED

SECURITY CLASSIFICATION OF THIS PAGE

REPORT DOCUMENTATION PAGE

1a. REPORT SECURITY CLASSIFICATION Unclassified		1b. RESTRICTIVE MARKINGS	
2a. SECURITY CLASSIFICATION AUTHORITY		3. DISTRIBUTION / AVAILABILITY OF REPORT Approved for public release; distribution unlimited.	
2b. DECLASSIFICATION / DOWNGRADING SCHEDULE		4. PERFORMING ORGANIZATION REPORT NUMBER(S) TR-0086(6935-07)-1	
5. MONITORING ORGANIZATION REPORT NUMBER(S) SD-TR-87-40		6a. NAME OF PERFORMING ORGANIZATION Laboratory Operations The Aerospace Corporation	
6b. OFFICE SYMBOL (If applicable)		7a. NAME OF MONITORING ORGANIZATION Space Division	
6c. ADDRESS (City, State, and ZIP Code) El Segundo, CA 90245-4691		7b. ADDRESS (City, State, and ZIP Code) Los Angeles Air Force Station Los Angeles, CA 90009-2960	
8a. NAME OF FUNDING / SPONSORING ORGANIZATION		8b. OFFICE SYMBOL (If applicable)	
9. PROCUREMENT INSTRUMENT IDENTIFICATION NUMBER F04701-85-C-0086		10. SOURCE OF FUNDING NUMBERS	
11. TITLE (Include Security Classification) The Synthesis and Characterization of Some Rare Earth Arsenides		PROGRAM ELEMENT NO	PROJECT NO.
12. PERSONAL AUTHOR(S) Schurr, Juliet N.		TASK NO	WORK UNIT ACCESSION NO.
13a. TYPE OF REPORT	13b. TIME COVERED FROM _____ TO _____	14. DATE OF REPORT (Year, Month, Day) 1987 September 10	15. PAGE COUNT 78
16. SUPPLEMENTARY NOTATION			
17. COSATI CODES		18. SUBJECT TERMS (Continue on reverse if necessary and identify by block number) Rare earth arsenides, Lattice parameter, Synthesis NdAs, Holmium neodymium, HoAs arsenide solid solution	
19. ABSTRACT (Continue on reverse if necessary and identify by block number) Solid solutions of a new material, $_{x}^{Nd}Nd_{1-x}^{As}As_{1-y}^{1-y}$ have been synthesized, and the binary arsenides NdAs and HoAs have been prepared. Chemical analyses have shown that both were arsenic deficient. Lattice parameters were determined for NdAs and HoAs and were found to be 5.995 Å and 5.768 Å, respectively. It has been established that a range of arsenic solubility exists in the binary arsenides where no change in lattice parameter is observed. High temperature thermal analyses were conducted on all arsenides. NdAs and HoAs exhibited arsenic volatilization upon heating, but $_{x}^{Nd}Nd_{1-x}^{As}As_{1-y}^{1-y}$ remained stable to 1000°C.			
20. DISTRIBUTION / AVAILABILITY OF ABSTRACT <input checked="" type="checkbox"/> UNCLASSIFIED/UNLIMITED <input type="checkbox"/> SAME AS RPT <input type="checkbox"/> DTIC USERS		21. ABSTRACT SECURITY CLASSIFICATION Unclassified	
22a. NAME OF RESPONSIBLE INDIVIDUAL		22b. TELEPHONE (Include Area Code)	22c. OFFICE SYMBOL

PREFACE

This research was performed in conjunction with a master's thesis project. I would therefore like to thank Dr. Bruce Dunn for his guidance as my graduate studies advisor at UCLA.

The following people at The Aerospace Corporation Materials Sciences Laboratory are acknowledged for their assistance: Paul Adams, x-ray diffraction; Joe Uht and Dick Brose, SEM/EDAX; Nick Marquez, IMMA; Bob Shenk, DSC; Steve Sandlin, TGA; and Bill McDermed, glasswork. In addition, support from the Material Physics Section, including George Panos, Ray Savedra and Ray Ruiz, is appreciated. Finally, Drs. Gary Hawkins, Jim Lhota II, and Wayne Stuckey should be credited with providing the impetus for this work.

Accession For	
NTIS CRA&I	<input checked="" type="checkbox"/>
DTIC TAB	<input type="checkbox"/>
Unannounced	<input type="checkbox"/>
Justification	
By _____	
Distribution/	
Availability Codes	
Dis:	Avail and/or Serial
A-1	

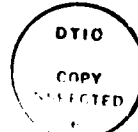


TABLE OF CONTENTS

	Page
PREFACE.....	1
CHAPTER 1 INTRODUCTION.....	9
CHAPTER 2 BACKGROUND.....	13
2.1 Specific Heat of NdAs.....	13
2.2 Previous Work on Other Rare Earth Systems.....	15
2.3 Preparation of Bulk Rare Earth Arsenides.....	19
2.3.1 Solid-Solid Reaction.....	20
2.3.2 Solid-Vapor Reaction.....	21
2.3.3 Preparation of Bulk Specimens.....	22
2.3.4 Crystal Growth.....	23
2.4 The Effect of Composition, Stoichiometry and Structure on Physical Properties of the Rare Earth Arsenides.....	24
CHAPTER 3 OBJECTIVE AND TECHNICAL APPROACH.....	27
CHAPTER 4 SYNTHESIS AND IDENTIFICATION OF THE ARSENIDES OF NEODYMIUM AND HOLMIUM.....	31
4.1 X-ray Analysis.....	31
4.1.1 Debye-Scherrer Method.....	31
4.1.2 Diffractometer Method.....	32
4.2 Chemical Analysis.....	33
4.3 NdAs and HoAs: Method of Preparation.....	35
4.3.1 NdAs: Results of Synthesis.....	38
4.3.2 HoAs: Results of Synthesis.....	42

4.4 $Ho_xNd_{1-x}As$: Methods of Preparation.....	45
4.4.1 $(Ho,Nd)As$: Results of Synthesis.....	46
4.4.2 $HoAs(Nd)$: Results of Synthesis.....	48
4.5 Determination of Lattice Parameter, a_0	54
4.5.1 Results of Lattice Parameter Measurements.....	56
CHAPTER 5 CHARACTERIZATION OF THE ARSENIDES OF NEODYMIUM AND HOLMIUM.....	61
5.1 NdAs Compatibility Tests.....	61
5.1.1 Results of NdAs Compatibility Tests.....	62
5.2 Thermogravimetric Analysis (TGA).....	63
5.2.1 Results of Thermogravimetric Analysis (TGA).....	64
5.3 Differential Scanning Calorimetry (DSC).....	67
5.3.1 Results of Differential Scanning Calorimetry (DSC).....	67
CHAPTER 6 DISCUSSION.....	71
6.1 Properties of $HoAs(Nd)$	71
6.2 Effects of Thermal Analysis on the Rare Earth Arsenides.....	74
6.3 Properties of NdAs and HoAs.....	76
CHAPTER 7 CONCLUSIONS.....	79
CHAPTER 8 FURTHER SUGGESTIONS FOR STUDY.....	81
REFERENCES.....	83

LIST OF FIGURES

	Page
2-1 Volumetric Heat Capacity of NdAs, He and Pb Versus Temperature.....	14
2-2 Temperature Dependence of the Specific Heat for Some Compounds of the Series $Gd_xEr_{1-x}Rh$	16
4-1 Schematic of a Quartz Tube Used in Compound Synthesis.....	36
4-2 Schematic of Furnace Arrangement.....	37
4-3 X-ray Diffractometer Charts of (a) NdAs#4 (b) (Ho, Nd)As#2 (c) HoAs#2.....	47
4-4 X-ray Diffractometer Charts of (a) HoAs#2(Nd) (b) HoAs#5(Nd) (c) HoAs#6(Nd).....	50
4-5 X-ray Diffractometer Charts of (a) NdAs#4 (b) HoAs#5(Nd) (c) HoAs#2.....	52
5-1 TGA in Argon (a) NdAs#3 (b) HoAs#1 (c) HoAs#5(Nd).....	65
5-2 DSC in Argon (a) NdAs#4 (b) HoAs#6 (c) HoAs#5(Nd).....	68
6-1 Lattice Parameter Versus Chemical Composition of $Ho_xNd_{1-x}As_{1-y}$	72
6-2 (a) Equilibrium Diagram of the As-Nd System (b) Intermediate Phase Formation in As-Nd System Near 50 Atomic % Nd.....	78

CHAPTER 1. INTRODUCTION

Cryogenic systems for space flight applications must be improved as low temperature cooling becomes a necessity for certain electronic devices. These devices contain various low temperature sensors which require cooling in a range between 1 and 100 K.

One type of cryogenic system under investigation is the mechanical refrigerators operating with a regenerative cycle. The regenerators in these cryocoolers function as small, efficient heat exchangers. They convert high temperature gas to low temperature gas by maintaining a temperature gradient across the regenerator matrix. Flowing through the regenerator, the gas is heated or cooled depending on the flow direction of the cycle. The matrix must be a good absorber of energy; that is, it must have a heat capacity which greatly exceeds that of the working gas for effective operation. In addition, it must have a very high heat transfer coefficient between itself and the gas along each point in the regenerator. However, the heat conductivity in the direction of gas flow must be low in order to minimize loss of heat or cold.

The regenerator matrix materials tested thus far include densely packed small lead balls and stacked phosphor bronze screens. The limitation in using these materials is that for cooling at temperatures approaching absolute zero, the heat capacity of the matrix also approaches zero, rendering the system increasingly inefficient. This situation underscores the need for research of new

regenerator materials for improving the present technology of cryogenic systems.

The objective of the present study is to synthesize new materials with large heat capacities per unit volume below 15 K. Making use of the fact that materials which undergo magnetic phase transitions may incur anomalously high values of specific heat at the transition temperatures, a search was conducted to determine which magnetic materials would be good candidates for further research. The rare earth compounds appeared promising as rare earth ions are known to undergo magnetic ordering. An extensive literature survey was conducted and a rare earth pnictide, neodymium arsenide (NdAs), that had a very large peak in specific heat near 11 K was found.⁽¹⁾ At this critical temperature, the Neel point, antiferromagnetic ordering occurs. However, for practical application in a regenerative cryocooler, it would be preferable for the matrix-material to retain its desirable property over a useful range of temperatures such as 1 to 15 K. This may be brought about if a solid solution is formed with NdAs and another rare earth compound which has a lower magnetic phase transition temperature than 11 K. It is expected that the new compound will exhibit a heat capacity which is lower than that of NdAs, but will span the applicable low temperature region.

Selecting the material to form a solid solution with NdAs also required taking into consideration various chemical properties including identical crystal structures, proximity in the periodic table and close values in atomic radii for the alloying element.

HoAs satisfies these requirements. It orders antiferromagnetically near 5 K and its easy direction of magnetization is the same as NdAs. In addition, it shares the same NaCl type crystal structure with NdAs. Finally, being another rare earth element, holmium is chemically similar to Nd and does not differ more than 15% in atomic radii. For these reasons, it appeared that the synthesis of the pseudobinary compound $Ho_xNd_{1-x}As$ was feasible.

This report describes the experimental procedure for the synthesis and characterization of NdAs, HoAs and the new compound, $Ho_xNd_{1-x}As$. The chemical, thermal and structural properties of these compounds are presented and discussed.

CHAPTER 2. BACKGROUND

2.1 SPECIFIC HEAT OF NdAs

The specific-heat anomaly of NdAs was first reported in 1973 by Aeby et al.⁽¹⁾ It was shown that a sharp peak in specific heat occurred at 10.6 K with a maximum value of $45 \frac{J}{K \cdot \text{mole}}$. Assuming NdAs has a fully close packed rocksalt structure, devoid of vacancies and its lattice parameter is 5.970 Å, as reported in the x-ray diffraction card files, the density of this compound is 6.844 g/cm³. The peak volumetric heat capacity is then calculated as approximately $1.4 \frac{J}{K \cdot \text{cm}^3}$.

The significance of knowing the heat capacity per unit volume becomes clearer upon examining the plot of volume specific heat of He, Pb and NdAs versus temperature (Figure 2-1). Helium is the typical working gas in a cryogenic refrigerator at an operating pressure of 20 atmospheres. The volume specific heat of He increases with decreasing temperature because the helium gas occupies less volume with decreasing temperature. As the helium gas liquifies, the specific heat begins to decrease with decreasing temperature. The specific heat per volume of lead, on the other hand, drops sharply below that of helium at approximately 15 K. Thus, lead loses its effectiveness as a regenerator matrix material below this temperature.

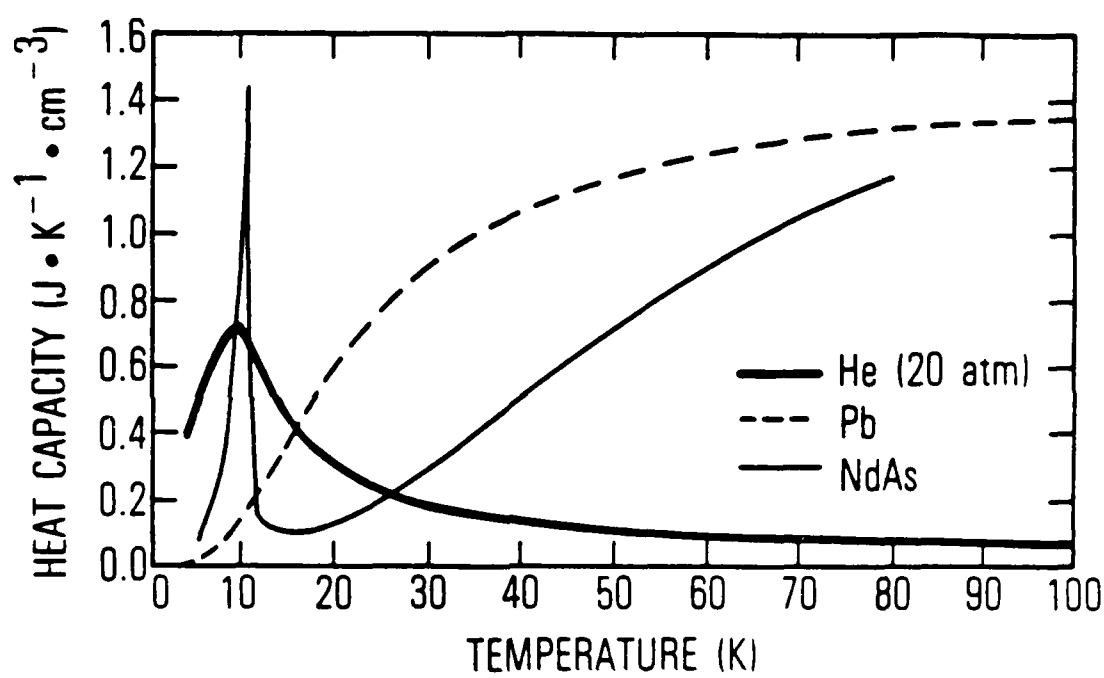


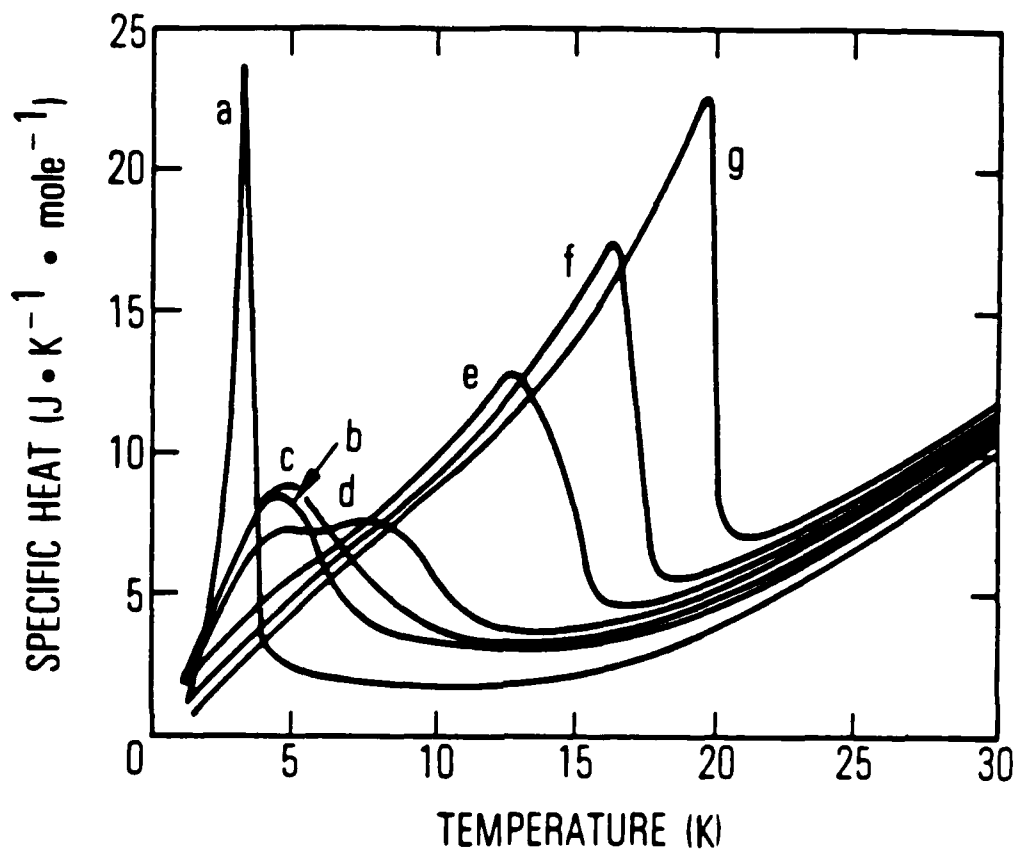
FIGURE 2-1. Volumetric Heat Capacity of NdAs⁽¹⁾, He⁽²⁾ and Pb⁽³⁾ Versus Temperature

The peak volumetric heat capacity of NdAs of $1.4 \frac{J}{K \cdot cm^3}$ is considerably larger than lead and the use of this material might provide a much improved regenerator near this one temperature. More desirable, however, would be a material whose high specific heat values covered a broader temperature range. A method of broadening the peak in specific heat will be discussed in the sections below.

2.2 PREVIOUS WORK ON OTHER RARE EARTH SYSTEMS

Previous experimental work reported by Buschow et al.⁽⁴⁾ demonstrated a method to reduce the magnetic transition temperature of a gadolinium compound by substituting other rare earth atoms, namely erbium, onto some of the Gd lattice sites. The pure binary compounds GdRh and ErRh have a T_c at 24.0 K and T_N at 3.2 K, respectively.

A series of $Gd_xEr_{1-x}Rh$ compounds was synthesized and their temperature dependence of specific heat was measured. Figure 2-2 shows that the maxima in the specific heat curves of the compounds with $0 < x < 1$ lie between those of the pure binary compounds. In addition, the specific heat anomaly broadened to over several degrees Kelvin.



a	ErRh	e	Gd _{0.8} Er _{0.2} Rh
b	Gd _{0.4} Er _{0.6} Rh	f	Gd _{0.9} Er _{0.1} Rh
c	Gd _{0.5} Er _{0.5} Rh	g	GdRh
d	Gd _{0.6} Er _{0.4} Rh		

FIGURE 2-2. Temperature Dependence of the Specific Heat for Some Compounds of the Series $Gd_xEr_{1-x}Rh^{(4)}$

The impetus for Buschow's work was similar to the present research, that is, to investigate materials with high volumetric heat capacity at low temperatures. Although the results were encouraging, one distinct disadvantage of this rare earth rhodium compound was the relatively high price of rhodium. Thus, a practical reason for pursuing the research of a $R_{1-x}Nd_xAs$ type compound (where R is another rare earth element) was that it might provide a less expensive regenerator material.

The properties of other rare earth arsenides were examined. Table 2-1 lists the temperature at which magnetic ordering occurs, the type of order and the easy direction of magnetization for nine rare earth arsenide compounds.

The Néel temperature of 12.5 K reported for NdAs was obtained by measuring the temperature dependence of magnetic susceptibilities. As stated earlier, specific heat measurements produced the 10.6 K value. The 13 K value was not referenced. NdAs orders anti-ferromagnetically with the magnetic moments pointing parallel to the 001 crystallographic direction.

Table 2-1. Magnetic Properties of Rare Earth Arsenides⁽⁵⁾

Compound	Magnetic Ordering Temperature	Type of Magnetic Order	Direction of Magnetic Moments (easy direction)
CeAs	$T_N = 7.5K, 5...7.5K$	Type I AFM	$\parallel[001]$
NdAs	$T_N = 13K, 12.5K, 10.6K$	Type I AFM	$\parallel[001]$
SmAs	$T_N = 1.8K$		
GdAs	$T_N = 25K$	Type II AFM	in [111]
TbAs	$T_N = 12K, 10.5K$	Type II AFM	$\parallel[111]$
DyAs	$T_C = 8.5K$	HoP type FM	
HoAs	$T_N = 4.8K$	Type II AFM	$\parallel[001]$
ErAs	$T_N = 3.5K, 2.9K$	Type II AFM	$\perp[111]$
YbAs	$T_N < 1.6K$		

Magnetic spins for CeAs and HoAs also align in this direction. In addition, they both have Neel temperatures (determined from magnetic measurements) lower than that of NdAs. However, as shown in Table 2-2, HoAs has a much higher density. This is a desirable property as it translates into a small molar volume per rare earth atom and a better opportunity for attaining a large specific heat per volume. No measurement of specific heat for HoAs could be found in the literature. Other physical properties of rare earth arsenides can be found in Table 2-2 including crystal structure and lattice parameter.

Table 2-2. Physical Properties of Rare Earth Arsenides

Compound	Crystal Structure	Lattice Parameter at Room Temperature, a_0 (Å)	Calculated Density (g/cm ³)
CeAs	NaCl	6.078, ⁽¹⁾ 6.072, ⁽⁶⁾ 6.0817 \pm 6 ⁽⁷⁾	6.38
NdAs	NaCl	5.994, ⁽¹⁾ 5.970, ⁽⁶⁾ 5.9953 \pm 3 ⁽⁷⁾	6.84
SmAs	NaCl	5.9205 \pm 4, ⁽⁷⁾ 5.921 ⁽⁸⁾	7.21
GdAs	NaCl	5.8659 \pm 1, ⁽⁷⁾ 5.862, ⁽⁹⁾ 5.854 ⁽¹⁰⁾	7.66
TbAs	NaCl	5.8244 \pm 3, ⁽⁷⁾ 5.827, ⁽⁹⁾ 5.813 ⁽¹⁰⁾	7.85
DyAs	NaCl	5.7933 \pm 4, ⁽⁷⁾ 5.803, ⁽⁹⁾ 5.780 ⁽¹⁰⁾	8.07
HoAs	NaCl	5.7687 \pm 4, ⁽⁷⁾ 5.771, ⁽⁹⁾ 5.759 ⁽¹⁰⁾	8.29
ErAs	NaCl	5.7427 \pm 3, ⁽⁷⁾ 5.745, ⁽⁹⁾ 5.732 ⁽¹⁰⁾	8.49
YbAs	NaCl	5.6979 \pm 4, ⁽⁷⁾ 5.702, ⁽⁹⁾ 5.698 ⁽¹⁰⁾	8.89

Table 2-3 lists some basic physical properties of the rare earth elements. Considering the ionic radii of holmium and neodymium, it can be presumed that either ion may substitute onto the other's lattice site as they are close in size and exhibit the same crystal structure.

2.3 PREPARATION OF RARE EARTH ARSENIDES

Several methods for the preparation of rare earth arsenides exist. In general, they involve the direct reaction of the elements in a solid-solid reaction or a solid-vapor reaction. Heating intimate mixtures of rare earth metal filings with powders or vapors of arsenic at temperatures between 300 and 1000°C produces a free-flowing granular compound. This material may then be used for the preparation of bulk crystalline specimens by powder metallurgical

techniques. In some cases, bulk specimens can be formed without the prereacted compound upon reacting bulk metal with arsenic vapor. Small crystals may be grown using an iodine vapor transport method or vapor deposition techniques. Each of these methods will be described.

Table 2-3. Physical Properties of Rare Earth Elements

Element	Atomic Number	Atomic Weight	Valence	Ionic Radii ⁽¹¹⁾ (Å)
Ce	58	140.12	Ce^{3+}	1.034
			Ce^{4+}	.941
Nd	60	144.24	Nd^{3+}	.995
Sm	62	150.35	Sm^{3+}	.964
			Sm^{2+}	1.143
Gd	64	157.25	Gd^{3+}	.938
Tb	65	158.92	Tb^{3+}	.923
Dy	66	162.50	Dy^{3+}	.908
Ho	67	164.93	Ho^{3+}	.894
Er	68	167.26	Er^{3+}	.881
Yb	70	173.04	Yb^{3+}	.858
			Yb^{2+}	1.02

2.3.1 Solid-Solid Reaction

This preparation procedure^(1,10,12,13,14,15) involves sealing a mixture of rare earth turnings and arsenic powder in an evacuated quartz tube and reacting by furnace heating. Serious consideration must be given to the heating rate of these mixed

powders as they may react with explosive violence if heated too rapidly between 250°C and the temperature range of reaction. A safe, controlled reaction can be achieved by following the conditions prescribed in Table 2-4, prepared from thermograms of dynamic differential calorimetry measurements. Also in the table are values of the heats of formation for some rare earth arsenides.

After reaching the upper limit of the reaction temperature range, the compound should be held at that level for several hours before raising the temperature up to 1000°C where further homogeneity can be obtained. At these higher temperatures, however, it is necessary to note that there is a possibility of the compound reacting with the silica tube in which it is contained. The rare earth arsenide synthesized is a granular compound of polycrystalline particles.

2.3.2 Solid-Vapor Reaction

Essentially similar to the solid-solid reaction, this preparation technique^(9,16,17) varies only in that the rare earth metal and the arsenic are physically separated by modifying the design of the silica ampoule. Here, arsenic vapor reacts with the rare earth filings and the occasion for a rapid, violent reaction to occur from the direct contact of the condensed phases is reduced.

Table 2-4. Reaction Conditions for the Measurement of Heats of Formation for Rare Earth Arsenides⁽¹³⁾

Metal	Heating Rate (°C/min)	Temperature Range in Which Onset of Reaction Was Noted		-ΔH kcal/mole at Reaction Temp.
		(°C)	(°C)	
Ce	1	330-335		69
Nd	1,2	345-385		73
Sm	1,2	335-375		72
Gd	2	365-455		74
Tb	2	380-470		75
Dy	2	395-575		78
Ho	2	305-415		72
Er	2	405-445		76
Yb	2	295-305		62

2.3.3 Preparation of Bulk Specimens

Because of the high melting points of the rare earth arsenides (typically > 2100°C) these compounds cannot readily be melted and cast into ingots. Instead, the powders can be pressed in the form of pellets and sintered. Unfortunately, a complete procedure defining what pressure, container material, atmosphere, reaction schedule, etc., to use could not be found for any one synthesis. Four available procedural descriptions, however, can be summarized as follows:

1. Press rare earth arsenide powder in the form of tablets, then heat under argon to 1100°C.⁽⁹⁾

2. Press rare earth at 100,000 psi, then sinter (2000° - 2500°C, 1/2 - 1 hr) in arsenic vapor. (17)
3. Recrystallize NdAs near 1800°C in molybdenum crucibles. (1)
4. Press CeAs into pellets 8-10 mm in height then heat to above 2200°C in sealed molybdenum or tungsten crucibles in order to recrystallize. (18)

Preparing bulk specimens using the solid-vapor reaction is possible by diffusing arsenic into sizable solid chunks of the rare earth metals at moderate temperatures. For example, at 750°C and with arsenic vapor pressure of 0.02 atmospheres, the reaction with neodymium metal proceeded to form a solid specimen of NdAs. (16)

2.3.4 Crystal Growth

When iodine is added to prereacted rare earth arsenide powders in a sealed and evacuated quartz ampoule and placed in a temperature gradient, crystal growth by iodide vapor transport occurs. (5,14,16) The quartz tube is usually 15-30 mm in inner diameter, 20-25 cm long and contains 1/100 - 5/100 mole of the arsenide compound. Hot zone temperatures in the 800 to 1150°C range are required so material transport can take place from the cold to the hot end. Small crystals (needles up to 5 mm or octahedra) are grown with this method. Crystal growth may also be accomplished by the sublimation of the rare earth arsenic compound in a closed

molybdenum or tungsten crucible.(18,19,20) In these reactions, heating temperatures above 2000°C are necessary. Differing results are reported for this experimental procedure. While crystals grown by Busch⁽¹⁹⁾ are homogeneous and stoichiometric, Hulliger and Ott⁽¹⁸⁾ report that preparing single crystals was quite difficult and some were slightly arsenic deficient.

2.4 THE EFFECT OF COMPOSITION, STOICHIOMETRY AND STRUCTURE ON PHYSICAL PROPERTIES OF THE RARE EARTH ARSENIDES

Several investigators report nonstoichiometric compositions of their compounds. As a result there are inconsistencies in the observed physical properties including electrical properties, magnetic ordering temperatures and lattice parameter values.(1,7,17,18,21) Table 2-5 lists some observed electrical properties of NdAs. Sample 42RA was prepared with excess arsenic and subsequently sintered in arsenic vapor at 1 atm pressure. The material was still slightly arsenic deficient as chemical analysis indicated a composition of Nd₁As_{.994}. The final composition of sample 46R was Nd₁As_{.96}. When comparing the carrier concentration values of these two samples, the suggestion has been proposed that lattice defects may be the source of high carrier concentrations. Indeed, Hulliger⁽²¹⁾ maintains that the synthesis of exact 1:1 stoichiometry rare earth pnictides (rare earth with group VA elements) is a problem because the compounds can exist over a certain range of compositions and that one percent excess of rare earth or deficit of anion would be sufficient to increase the free electron concentration to cause a metallic behavior in these valence

Table 2-5. Electrical Properties of Some NdAs Samples⁽¹⁷⁾

Sample	Synthetic Composition	Temperature (°C)	Resistivity (ρ, 10^{-3} ohm·cm)	Carrier Concentration (n, 10^{20} cm^{-3})
42R	NdAs	310	.21	4.0
		97	.12	4.2
42RA	NdAs	309	.155	4.7
		102	.054	4.3
29R	NdAs	304	.142	5.2
		106	.087	5.2
46R	NdAs	300	.15	12

compounds. This metallic characteristic is fortuitous as it would lead to the high thermal conductivity that is necessary for quick heat exchange.

Lattice parameter measurements can also give some indication as to the stoichiometry of a compound. Compounds with cation and/or anion vacancies may have smaller a_0 values while those nearer the ideal stoichiometry will have a larger lattice constant. This, of course, assumes that neither interstitials nor foreign impurities are entering the structure. On the other hand, Taylor et al.⁽⁷⁾ report that variations in arsenic content can occur in certain rare earth arsenides with no detectable change in lattice parameters. A list of various lattice parameter values was given in Table 2-2. In addition, the different magnetic ordering temperatures reported in the literature (shown previously in Table 2-1) seem to be caused by varying stoichiometry in the samples.⁽¹⁾ Thus, the specific heat maxima may be sensitive to structural imperfections, to the presence of impurities, and to the overall stoichiometry of the samples.

CHAPTER 3. OBJECTIVE AND TECHNICAL APPROACH

The objective of this study is to synthesize and characterize a solid solution of $Ho_xNd_{1-x}As$, a new material which is expected to have a large volume heat capacity across the 5 to 10 K temperature range. In addition, the synthesis and characterization of NdAs and HoAs are important prerequisites for studying $Ho_xNd_{1-x}As$. X-ray diffraction analysis, chemical analysis, thermogravimetric analysis and differential scanning calorimetry will be performed in order to characterize the above materials.

The synthesis of the $Ho_xNd_{1-x}As$ solid solution will be pursued by attempting to substitute Ho atoms onto the Nd lattice sites in NdAs or Nd atoms onto the Ho lattice sites in HoAs. Of the methods to be tried for the synthesis of $Ho_xNd_{1-x}As$, the first method will be to follow a procedure similar to the one used in the preparation of NdAs and HoAs. Therefore, the safe, successful synthesis of these pure binary compounds must initially be achieved in order to confirm that the method of preparation is valid and reproducible. A commercially available (CERAC, Inc.) NdAs compound will be obtained for purposes of comparison with the synthesized NdAs. Once these reactions are satisfactorily completed, the method for preparing the binary compound will be used to prepare the holmium neodymium arsenide. Another method to be attempted entails reacting HoAs with a melt of neodymium metal. This liquid-solid reaction may provide an increased diffusion rate of the substitutional atoms compared to the rate of diffusion in the solid state reaction.

All compounds formed will be analyzed by a variety of techniques. X-ray diffraction analysis will be used to identify the compounds present in the product. The results of the analysis will prove whether the arsenide did indeed form, whether by-products from any reaction with the container material are present and whether any other impurities exist. Furthermore, x-ray analysis will provide the means to determine lattice parameters of the arsenide compounds. Precise lattice parameter values of the samples will indicate the variations from synthesis to synthesis as well as provide comparisons with values for lattice parameters reported in the literature. The prevailing reason for determining the lattice parameters of the holmium neodymium arsenide compounds is to detect a shift in the diffraction lines. A shift would result if there were an incorporation of Nd or Ho atoms respectively into the HoAs or NdAs lattice, thereby expanding or contracting the unit cell.

Analysis of the chemical compositions of the samples will determine the impurity content and indicate the stoichiometry. Since the detection limits of x-ray analysis are on the order of a few percent, the Ion Microprobe Mass Analyzer (IMMA) will be utilized to provide low level impurity identification of a large number of possible elements. In particular, handling contaminants such as sodium, calcium and potassium can be monitored as well as hydrogen and oxygen content from oxide and hydroxide formation. The energy dispersive x-ray spectrometer (EDXS) attachment on the scanning electron microscope (SEM) with associated computer aid can analyze small amounts of sample for semiquantitative elemental composition

(elements with atomic number greater than 11) in a nondestructive manner. The EDXS will be used to analyze the chemical content of small particles. Finally, for more precise knowledge of stoichiometry, chemical analysis using an indirectly coupled plasma-atomic emission spectrometer (ICP-AES) will be used.

The high temperature thermal characteristics of the arsenide compounds will be examined by performing thermogravimetric analysis (TGA) and differential scanning calorimetry (DSC). Since all materials ultimately decompose upon heating and their decomposition temperature is a characteristic property of each material, TGA yields information about the thermal stability of the compound. DSC can also be applied to determine thermal stability and to characterize phase transitions or chemical reactions. The results of TGA and DSC analysis may give insight to the similarities and differences among the various rare earth arsenide compounds synthesized.

Finally, in anticipation of measuring specific heat of these compounds in the future, the preparation of bulk specimens will be investigated. Container materials compatible with NdAs at high temperatures will be surveyed. From the results of the compatibility tests and the thermal analyses, a procedure for forming bulk specimens can be designed and implemented.

CHAPTER 4. SYNTHESIS AND IDENTIFICATION OF THE ARSENIDES OF NEODYMIUM AND HOLMIUM

4.1 X-RAY ANALYSIS

X-ray diffraction analysis is one of the necessary tools for compound identification, lattice parameter measurements, and the detection of solid solution formation or change in composition. Both the photographic method using the Debye-Scherrer camera and the diffractometer technique were utilized in order to take advantage of the particular benefits of each method.

4.1.1 Debye-Scherrer Method

The standard Debye-Scherrer camera for powder specimens was employed using CuK α radiation and a nickel filter. The powder camera is superior to a diffractometer when only a very small amount of material is available. The powder camera was also the most readily accessible instrument during the early stages of this research. For compound identification, a 0.5 mm glass capillary was filled with a small amount of powder (~ 1 mg) which was crushed in a mortar and pestle prior to sampling. This ensured that the sampling was representative of the entire compound. The sample was placed on the axis of the cylindrical camera and aligned with the x-ray beam. Film exposure times ranged from 2 to 4 hours.

A small diameter (0.3 mm) capillary was used to produce sharp diffraction lines for conducting lattice parameter measurements. Diffraction lines originating from lattice planes with large Bragg angles, θ , can be determined more accurately by film

methods than by diffractometer techniques. In addition, the simple apparatus of the Debye-Scherrer method makes it less subject to misalignment errors than the diffractometer. For these reasons, the Debye-Scherrer method was the preferred choice for use in lattice parameter determinations.

4.1.2 Diffractometer Method

When, for some samples, diffraction lines on the film became too broad and indistinguishable for meaningful analysis, a vertical Philips diffractometer was used. In the diffractometer method, the intensity of the diffracted x-ray beam is measured directly by an electronic counter rather than by the blackening of photographic film. A strip chart recorder graphically plots the output of intensity versus 2θ . Thus, what appears on the film as a broadened line manifests itself on chart paper as a distinct, but broad peak which extends across a range of 2θ .

Sample preparation for this method required making an acetone slurry with 30 to 40 mg of finely crushed powder. The slurry was deposited on the quartz window section of an aluminum sample holder. The acetone was allowed to evaporate leaving a thin layer of powder adhering to the quartz surface. The sample was exposed to copper radiation and the diffracted beam passed through a graphite crystal monochromator which allowed only $K\alpha$ radiation to reach the counter. Typically, the diffractometer was operated at a scanning rate of 2° per minute and the diffracted intensity over an angular range from 7° to 120° was measured. Values of 2θ were read directly

off the strip chart recorder for calculation of d values.

4.2 CHEMICAL ANALYSIS

Three forms of chemical analysis were performed for the qualitative, semiquantitative and quantitative determinations of chemical composition of the samples. They include the IMMA, the EDXS on the SEM and the ICP-AES.

The IMMA is an instrument which provides mass analysis of the surface layers of solid samples by bombarding the material surface with a beam of high energy oxygen ions. These primary ions strip off the upper atomic layers of the sample, producing some secondary ions which are then collected into a mass spectrometer and analyzed according to their mass-charge ratio. The small sample particles which were analyzed in this study were pressed into a piece of soft indium metal which in turn was pressed on an aluminum sample holder. This analytical method can detect the presence of nearly all elements in the periodic table down to trace quantities. Exceptional sensitivities (ppm) can be obtained for easily ionizable elements such as sodium, calcium, potassium, etc. This method of chemical analysis will be used to identify elements present in the sample.

The EDXS is an attachment on the SEM which provides energy dispersive x-ray analysis of specimens. When electrons from the primary beam of the SEM impinge on a specimen, specimen electrons are ejected from their energy levels. Electron vacancies occurring in low energy inner levels allow electrons from higher energy outer levels to fill

their places, releasing energy as x-rays. These x-rays have energies characteristic of the elements from which they emanate. The EDXS separates the x-rays according to these energies. Because the relative intensities of the x-rays produced are not necessarily equal to the relative abundance of the atoms producing the x-rays, an exact quantitative analysis of elemental composition of a sample is not possible. However, with the development of computer processing of EDXS data, programs that include correction factors to compensate for some of the parameters which affect relative intensities of x-rays other than elemental abundance are available. These computer programs have been utilized to provide rapid, semiquantitative analyses of specimens.

The sample holder used for this analysis was a graphite disk with its flat surface covered with double-sided adhesive tape. A few particles of powdered sample were placed on the tape. The electron beam bombarded a small area of the particles and the elemental composition of that region was determined.

For quantitative analysis, an ICP-AES from Geochemical Services, Inc. (Torrance, CA) was used. In an ICP-AES, a very high temperature argon plasma provides the heat necessary to dissociate and excite the atoms in a compound. Characteristic radiation from the excited atoms is emitted in proportion to the concentration of the elements in the sample. Thus, the quantity of an element present can be accurately determined particularly if standard solutions of the element in question are used as references in the analysis. Preparation of the samples for these analyses required dissolving an accurately weighed

amount of powder (at least 50 mg) in aqua regia and diluting it with deionized water to a known volume. All of the sample was consumed in the acid digestion, and each sample was analyzed three times.

4.3 NdAs AND HoAs: METHOD OF PREPARATION

The solid-solid reaction procedure described in Chapter 2 was used to prepare these two arsenide compounds. Stoichiometric proportions of pure rare earth turnings, either Nd or Ho (-40 mesh 99.9%), and arsenic powder (99.9999%) were weighed and funnelled into a quartz tube. The quartz tubes are typically 1 cm in diameter and 10 cm long (Figure 4-1). This was performed in an argon filled glovebox. In later syntheses, arsenic chunks were substituted for the powder to slow down any oxidation in the arsenic starting material; this proved to be satisfactory for the reaction as well.

The quartz ampoule was then transferred to a vacuum system and evacuated to 10^{-6} torr for about 1/2 hour. While under a vacuum, the tube was pinched closed with a torch, being careful to keep the reactants cool. To prevent heat from travelling towards the powder at the bottom of the tubes, each quartz ampoule was designed with a "maria", a bulge formed in the tube immediately below the pinchoff area. After closure, the reactants were ready for synthesis. The quartz ampoule was placed in an upright position within a mullite tube, which can be safely heated to a maximum of 1700°C. The assembly was then heated in a programmable ashing furnace as shown in Figure 4-2.

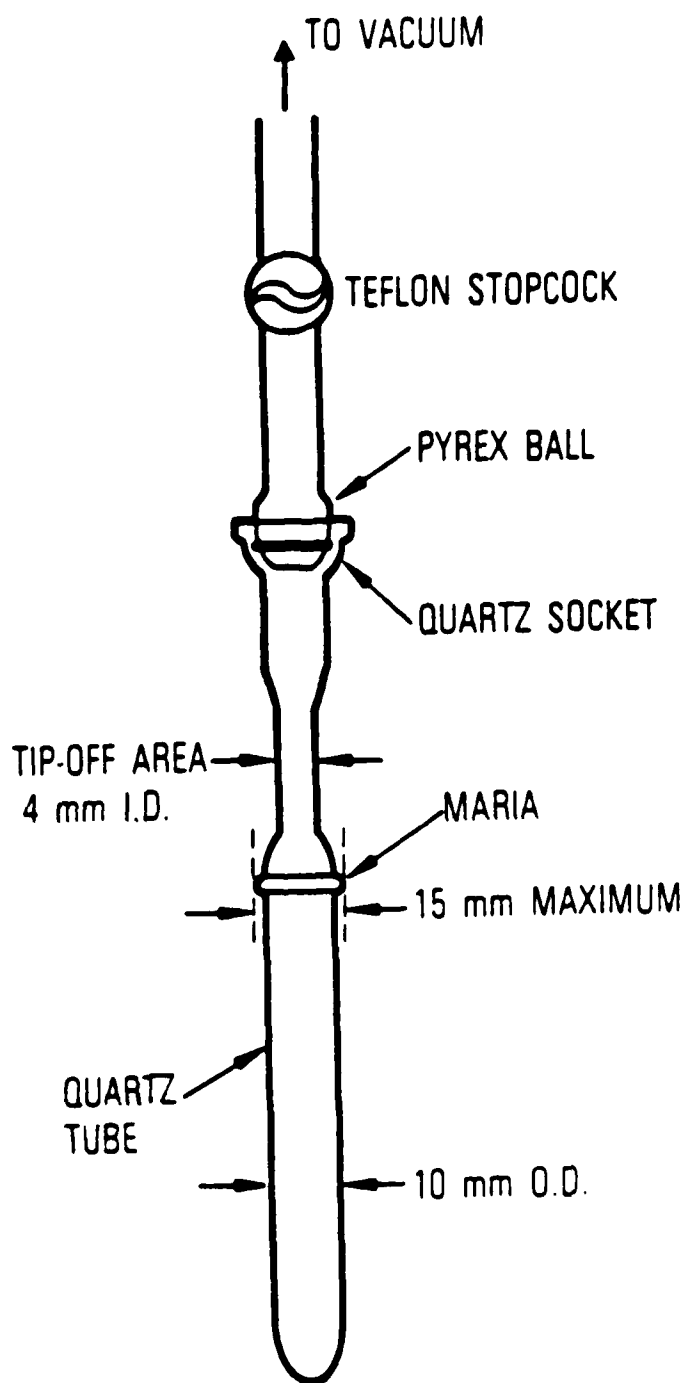


FIGURE 4-1. Schematic of a Quartz Tube Used in Compound Synthesis

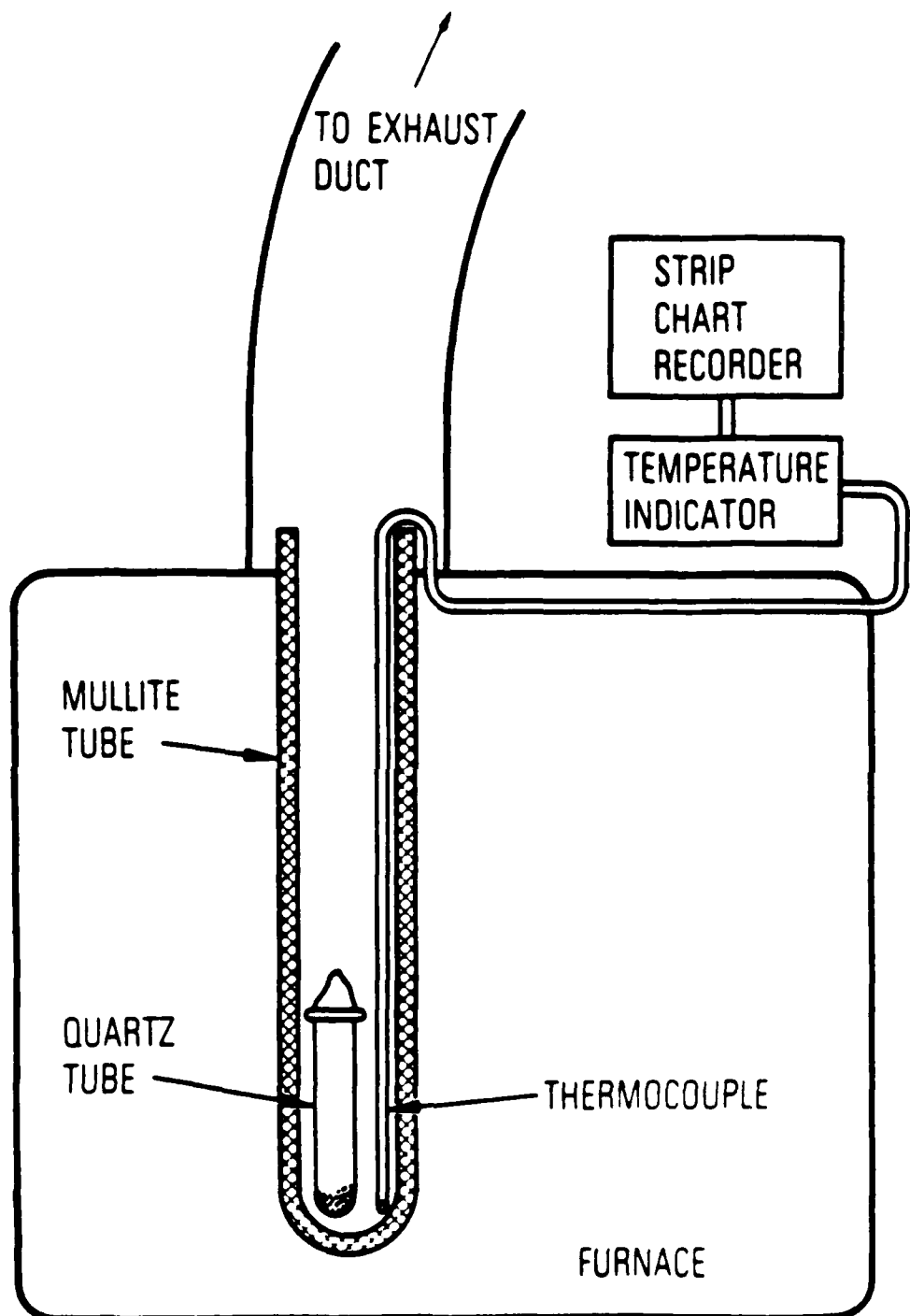


FIGURE 4-2. Schematic of Furnace Arrangement

Although the furnace had internal thermocouples of its own, additional thermocouples were inserted to check the actual temperature directly adjacent to the powders and to monitor the programmed heating schedule with a strip chart recorder. Safety precautions warranted having the open end of the mullite tube connected to an exhaust duct in case the quartz tube exploded.

Typical temperature-time parameters for the reaction were as follows:

<u>Temperature</u>	<u>Rate</u>
R.T. to 240°C	10 or 15°C/min
240 to 440°C	1°C/min
440°C	4 hr hold
440 to 910°C	5 or 10°C/min
910°C	4 hr hold

At the end of the reaction, all samples were allowed to cool naturally in the furnace.

4.3.1 NdAs: Results of Synthesis

Six lots of NdAs were safely and successfully prepared. The data are summarized in Table 4-1. The x-ray patterns of the first five syntheses were distinct and showed no other lines than those which agreed with NdAs crystals. In contrast, the x-ray pattern of the NdAs powder purchased from CERAC, Inc. was not as sharp and revealed additional diffraction lines corresponding to Nd(OH)_3 . The CERAC NdAs was a very fine dark grey powder. NdAs #1

through #6 appeared more like the original Nd metal reactant; however, the product was more brittle and darker in color. That is, the synthesized NdAs particles were small, dark gray to black turnings that crumbled easily when crushed.

Table 4-1. Synthesis of NdAs Compounds

Sample	Weight of Reactants (mg)		Identification of Product by X-ray Analysis	Deposit at Top of Tube	X-ray of Deposit
	Nd	As			
NdAs #1	30	15	NdAs	did not observe	X
NdAs #2	60	30	NdAs	yes, some	As
NdAs #3	80	40	NdAs	yes, some	X
NdAs #4	200	100	NdAs Diffractometer: NdAs	yes, some	X
NdAs #5 ^a	200	100	NdAs	very little to none	X
NdAs #6 ^b	--	--	--	--	--
NdAs #7	190	100	X	yes, small specks	X
CERAC NdAs ^c			NdAs, Nd(OH) ₃	--	--

X not determined

-- does not apply

^a This sample was heat treated a second time before opening the quartz tube. It was heated rapidly (25°C/min) to 1100°C and held for 5 hours before allowing to cool.

^b The quartz tube was not successfully pinched closed and the reaction was aborted.

^c CERAC NdAs refers to the powdered NdAs compound purchased from CERAC, Inc., Milwaukee, Wisconsin.

One sample, NdAs #5, was heated a second time to a high temperature (1100°C) to determine if a longer heat treatment would compact the powders into one solid mass. Although the particles did agglomerate, the sample was observed to be very loosely packed and crumbled immediately upon handling. The quartz tube was clouded over and appeared attacked by the NdAs. In all the other syntheses, the quartz tubes remained clear.

The quartz tubes used in all of the early syntheses were approximately 10 cm long. Deposits of a shiny, silver-colored material were found in varying amounts at the top of these tubes. X-ray diffraction of the deposit from NdAs #2 indicated this deposit was pure arsenic. Ensuing syntheses were carried out in 8 cm long quartz tubes in order to reduce the temperature gradient across the length of the tube. This modification helped but did not always eliminate the arsenic deposition. The arsenic may either be an excess amount not required in the reaction or material which did not react with the rare earth turnings, thereby producing an arsenic deficient compound. The source of these arsenic deposits was not fully determined.

Results of the chemical analyses are listed in Table 4-2. The IMMA results showed that NdAs #1 had some H, O, Mg and Si impurities. The CERAC NdAs contained, in addition to those impurities, a notable presence of Al and the handling contaminants Na, Ca and K. When analyzed by the EDXS, NdAs #3, #4, and #5 were determined to be composed of 47% As and 53% Nd (all percentages refer to mole percent). The detection of 7% Ag in NdAs #3 in the analysis

could not be explained. The Si content of these samples was not investigated. It was shown by atomic emission spectroscopy, however, that the Si content of NdAs #4 was 0.2%. The remaining composition of NdAs #4 was 50.8% Nd and 49.0% As. EDXS and AES values for the CERAC NdAs were in substantial agreement. The As concentration was determined by AES to be 43.3% and the Nd concentration was 55.3%. The remaining 1.4% was silicon.

Table 4-2. Chemical Analysis of NdAs Compounds

Sample	Type of Analysis	Results [†]		
NdAs #1	IMMA	H, O, Mg, Si, As, Nd		
CERAC NdAs	IMMA	H, O, Na, Mg, Al, Si, K, Ca, As, Nd		
NdAs #3	EDXS	Nd: 46%	As: 47%	Si: X (Ag ~ 7%)
NdAs #4	EDXS	53%	47%	X
NdAs #5	EDXS	54%	46%	X
	EDXS	54%	47%	X
CERAC NdAs	EDXS	54%	43%	3%
	EDXS	55%	44%	1%
	EDXS	56%	43%	1%
NdAs #4	ICP-AES	50.8%	49.0%	0.2%
CERAC NdAs	ICP-AES	55.3%	43.3%	1.4%

X not determined

† all percentages refer to mole percent

The method used to perform the NdAs synthesis provided good, repeatable results and was considered satisfactory for similar synthesis of HoAs.

4.3.2 HoAs: Results of Synthesis

Seven lots of HoAs were prepared. These are summarized in Table 4-3. These lots also had arsenic deposits at the top of the quartz tube. The HoAs particles, however, were neither all black nor dark grey like those of the NdAs syntheses. Some appeared to be shiny or light grey in color. Several samples of HoAs contained Ho_2O_3 , as revealed by x-ray diffraction analysis. The x-ray patterns which appeared for Ho_2O_3 never included more than the 4 or 5 major peaks of Ho_2O_3 and all of the peaks were weak in intensity. The HoAs pattern was especially sharp, well resolved and dark in intensity. When an EDXS analysis (Table 4-4) was performed on a black particle and a shiny particle separately, the result disclosed that both kinds of particles had nearly the same concentration of Ho to As, namely ~ 58% to 42%.

Other HoAs samples showed nonstoichiometric proportions of Ho to As. The synthesis of HoAs #5 and HoAs #6 was modified to lengthen the time allowed for the low temperature reaction as well as to increase the high temperature hold time. These samples were the first ones to utilize As chunks as opposed to As powder in the reaction. The chemical analysis of these samples by EDXS analysis indicated a slightly increased As concentration although the compound was still several percent As deficient for stoichiometry. No Ho_2O_3 was detected by x-ray analysis. HoAs #7 also incorporated a change in synthesis procedure. Here, the As to Ho ratio of reactants was doubled from 1:1 to 2:1 with a heat treatment cycle similar to that of HoAs #5. Again, it appeared from EDXS analysis that a greater

arsenic concentration occurred in the product compared to HoAs #1, 2, or 3. The large arsenic chunk deposited at the top of the tube weighed approximately 80 mg, which corresponded closely to the excess 1 millimole of As which was added beyond that which was necessary for stoichiometry.

Table 4-3. Synthesis of HoAs Compounds

Sample	Weight of Reactants (mg)		X-Ray Analysis of Product	Deposit at Top of Tube	X-ray of Deposit
	Ho	As			
HoAs #1	82	37	HoAs(Ho ₂ O ₃)	yes, little	As,(As ₂ O ₃)
HoAs #2	165	75	HoAs(Ho ₂ O ₃)	yes, clumps	X
HoAs #3 ^a	200	90	HoAs	yes, many specks	X
HoAs #4	206	93	X	yes, clumps	X
HoAs #5 ^b	250	110	HoAs	yes, small needles	X
HoAs #6 ^b	330	150	HoAs	yes, several small chunks	X
HoAs #7 ^{b,c}	330	225	HoAs(Ho ₂ O ₃)	yes, large chunks (~ 80 mg)	X

X Not determined.

^aThis sample was heat treated a second time before the quartz tube was opened. It was heated rapidly (25°C/min) to 1100°C and held there for 8 hours before being allowed to cool.

^bLonger reaction time (typically 1°C/min from 240°C to 600°C), longer hold time at 1000°C (300 min).

^cThis sample was prepared with a Ho to As ratio of 1:2, that is, an excess amount of arsenic.

Table 4-4. Chemical Analysis of HoAs Compounds

Sample	Type of Analysis	Results [†]			Notes
HoAs #1	EDXS	Ho: 56%	As: 42%	Si: X	(< 2% Ag) (black particle)
	EDXS	59%	41%	X	(shiny particle)
HoAs #2	EDXS	58%	42%	X	(black particle)
HoAs #3 ^a	EDXS	57%	43%	X	
	EDXS	59%	41%	X	
	EDXS	59%	41%	X	
HoAs #5 ^b	EDXS	56%	44%	X	
	EDXS	55%	45%	X	
HoAs #6 ^b	EDXS	56%	43%	1%	
	EDXS	53%	44%	3%	
HoAs #7 ^{b,c}	EDXS	54%	45%	< 2%	
	EDXS	54%	45%	1%	
HoAs #6	ICP-AES	58.5%	41.4%	0.1%	

[†] all percentages are in mole %

X Not determined

^a heat treated twice

^b longer reaction time (typically 1°C/min from 240 to 600°C);
longer hold time at 1000°C (300 min)

^c ratio of reactants - Ho to As, 1:2

The HoAs #3 synthesis, which included a second heat treatment after the original reaction, demonstrated that a long hold (8 hours) at 1100°C leads to the degradation of the quartz container. Furthermore, the product remained in a particulate form and no clumping or sintering was observed. HoAs #6 was the only HoAs sample inspected with atomic emission spectroscopy. The results differed somewhat from the EDXS values but were still quite consistent. AES indicated a larger Ho concentration and a silicon content of 0.1%.

4.4 $Ho_xNd_{1-x}As$: METHODS OF PREPARATION

Two methods of preparation were attempted for the synthesis of the $Ho_xNd_{1-x}As$ alloy. The first method followed the above solid-solid reaction procedure with the exception that a given ratio of holmium to neodymium was used. These were referred to as the $(Ho,Nd)As$ syntheses.

The second method entailed synthesizing a quantity of HoAs then reacting it with Nd at a temperature above the melting point of the Nd metal ($1021^{\circ}C$). This procedure also utilized the quartz tube arrangement. The furnace schedule was altered allowing for the HoAs to remain in a pool of molten rare earth metal. The samples were called the $HoAs(Nd)$ compounds. Note that the opposite combination of reacting NdAs with Ho was not feasible in the quartz ampoule as Ho required a melting temperature of $1470^{\circ}C$; the annealing point of clear fused quartz is $1140^{\circ}C$. Typical temperature-time parameters for the second method were as follows:

<u>Temperature</u>	<u>Rate</u>
R.T. to $1000^{\circ}C$	10,15 or $20^{\circ}C/min$
$1000^{\circ}C$	hold 5, 10 min
1000 to $1050^{\circ}C$	5, $10^{\circ}C/min$
$1050^{\circ}C$	#2 240 min (4 hr)
	#3 720 min (12 hr)
	#5 720 min (12 hr)
	#6 2880 min (48 hr)

4.4.1 (Ho,Nd)As: Results of Synthesis

Various mole ratios of Ho to Nd reactants were used to prepare the (Ho,Nd)As compounds. The ratios included 1:99, 10:90, 50:50, 90:10, and 99:1 mole percent Ho to Nd. In every case, x-ray analysis established that a single phase with a $Ho_xNd_{1-x}As$ composition did not form. Instead, both NdAs and HoAs were present in a physical mixture as evidenced by sharp, distinct diffraction patterns for each of the two phases. Several weak diffraction lines corresponding to Ho_2O_3 were also identified in the x-ray analysis of all syntheses except one. Arsenic deposits were observed for most samples and, in one case, the deposit weighed approximately 6 mg.

Figures 4-3 a, b, c provide a comparison of the x-ray diffractometer patterns of NdAs, (Ho,Nd)As and HoAs. In the (Ho,Nd)As pattern, each of the rare earth arsenide lines corresponds to either a NdAs or HoAs diffraction line. Thus, it has been clearly established that this method did not lead to the formation of the desired $Ho_xNd_{1-x}As$ compound.

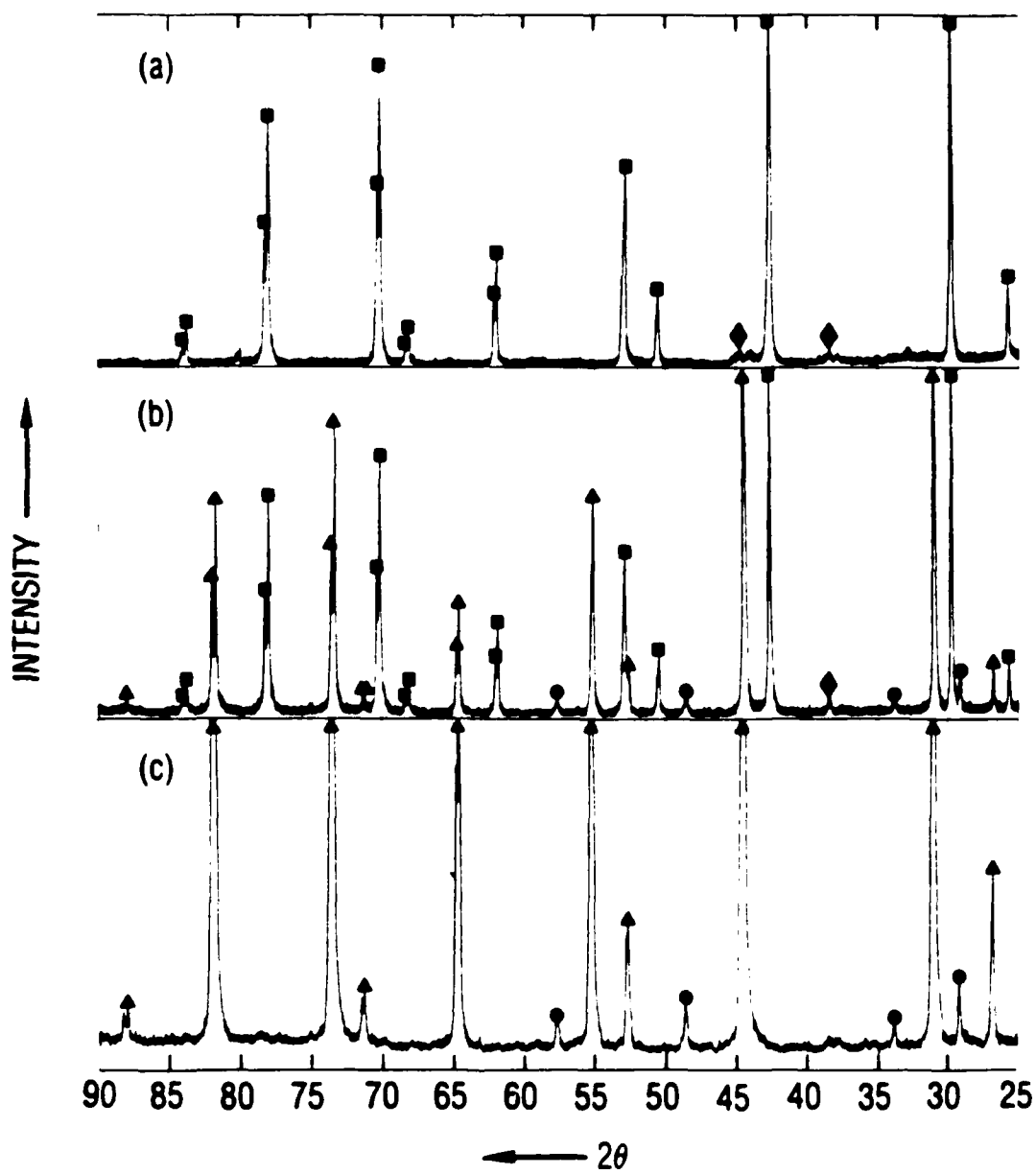


FIGURE 4-3. X-ray Diffractometer Charts of
 (a) NdAs#4
 (b) (Bo,Nd)As#2
 (c) HoAs#2

NdAs ■ Al ♦ Ho_2O_3 • HoAs ▲

4.4.2 HoAs(Nd): Results of Synthesis

The preparation of four different HoAs(Nd) syntheses was accomplished. Each batch differed from the others by having various amounts of HoAs and Nd reactants in the starting composition and by varying the final high temperature soak time from 4 to 48 hours as reported in Section 4.4. The Ho to Nd ratios in HoAs#2(Nd), HoAs#3(Nd), HoAs#5(Nd) and HoAs#6(Nd) were 1:0.8, 1:0.7, 1:0.5, and 1:0.5 respectively prior to the reaction. HoAs(Nd) products appeared to be composed of two distinct constituents. The first constituent (#1) was a partially sintered, hard, dark gray mass. The second constituent (#2) was a thin, grey, brittle material that formed around constituent #1. X-ray diffraction analysis of constituent #2 of HoAs#2(Nd) revealed that it was made up of a complex mixture of Ho_2O_3 , HoAs, Ho_5Si_3 , HoSi and possibly some Nd_5Si_4 . Having reacted with the rare earth compounds, the bottom of the quartz tube was no longer clear but rather an opaque white.

Constituent #1 of HoAs#2(Nd) was analyzed by both the Debye Scherrer and the diffractometer methods. Broad bands instead of sharp lines appeared on the x-ray film. Each band was located between the line positions associated with the HoAs and NdAs patterns. Similarly, broad asymmetric peaks positioned between the HoAs and NdAs peaks were recorded on the strip chart paper of the diffractometer. The broad nature of the peaks showed that the compound existed over a range of compositions. The asymmetric shape of the diffractometer peaks indicated that the various compositions were present in varying concentrations relative to the height of the

curve. A number of the major peaks even had small shoulder peaks on the one side of the curve. These shoulders also pointed to the inhomogeneous composition of HoAs#2(Nd). Figure 4-4a is part of the diffractometer pattern of HoAs#2(Nd).

Constituent #1 of HoAs#3(Nd), HoAs#5(Nd), and HoAs#6(Nd) was analyzed with the diffractometer and also produced broad diffraction peaks. Although the ratio of Nd to Ho was reduced somewhat in the HoAs#3(Nd) compared with the HoAs#2(Nd) synthesis, because of the longer high temperature hold (12 hr instead of 4 hr) the diffraction pattern indicated a greater incorporation of Nd into the $Ho_xNd_{1-x}As$ product. The peaks were shifted towards the NdAs peak positions. When less Nd reactant relative to Ho was used and the furnace schedule was unchanged with respect to the 12 hour hold period, the diffraction peaks moved back toward the HoAs direction as discovered in the HoAs#5(Nd) synthesis. Finally, maintaining the same Ho to Nd ratio as HoAs #5(Nd), HoAs#6(Nd) was reacted with a 48 hr high temperature hold. The diffractometer analysis for HoAs#6(Nd) revealed that HoAs was the compound present in the largest quantity and not the $Ho_xNd_{1-x}As$ composition. In addition, the increased Ho_2O_3 concentration in HoAs#6(Nd) manifested itself in sharp diffraction peaks of greater intensity.

Figures 4-4 b and c include part of the diffractometer patterns for HoAs#5(Nd) and HoAs#6(Nd). The shifting of the peaks due to varying the reaction conditions can be seen. The small Al peaks found in some diffraction patterns originate from the Al sample holder and may be disregarded.

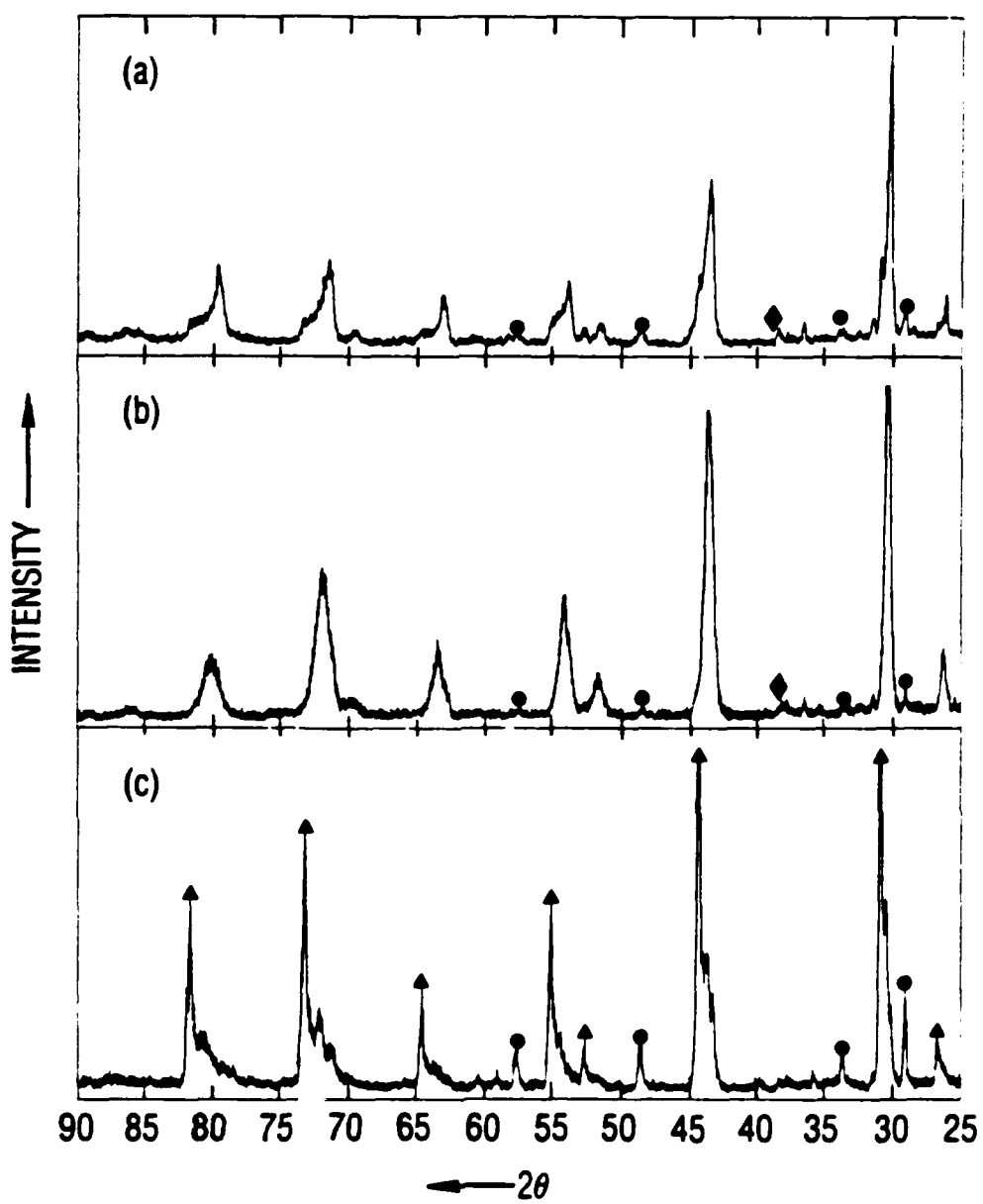


FIGURE 4-4. X-ray Diffractometer Charts of

- (a) HoAs#2(Nd)
- (b) HoAs#5(Nd)
- (c) HoAs#6(Nd)

Ho_2O_3 \bullet Al \blacklozenge HoAs \blacktriangle

In Figures 4-5 a, b, and c, the HoAs#5(Nd) pattern is reproduced as well as the NdAs and HoAs diffractometer patterns. By comparing these patterns, it was confirmed conclusively that a $Ho_xNd_{1-x}As$ solid solution had been synthesized. All the diffraction peaks of HoAs#5(Nd) fall within the boundaries of the two binary rare earth arsenides.

Chemical analyses of these four syntheses by EDXS (Table 4-5) supports the results obtained from the diffractometer analysis. It is clear that the shifting of the diffraction peaks arises from a change in chemical composition. HoAs#3(Nd) had the highest concentration of Nd followed by HoAs#2(Nd) then HoAs#5(Nd). The particles of HoAs#6(Nd) analyzed by EDXS were found to contain very little to no Nd. It was determined that all HoAs(Nd) solid solutions contained no more than 45 mole % arsenic. Atomic emission spectroscopy analysis performed on HoAs#5(Nd) corroborated the EDXS results of the same compound to within three percent. This is a similar level of agreement as was observed with HoAs compounds (Table 4-4). The silicon content in HoAs#5(Nd) was found to be 0.2%.

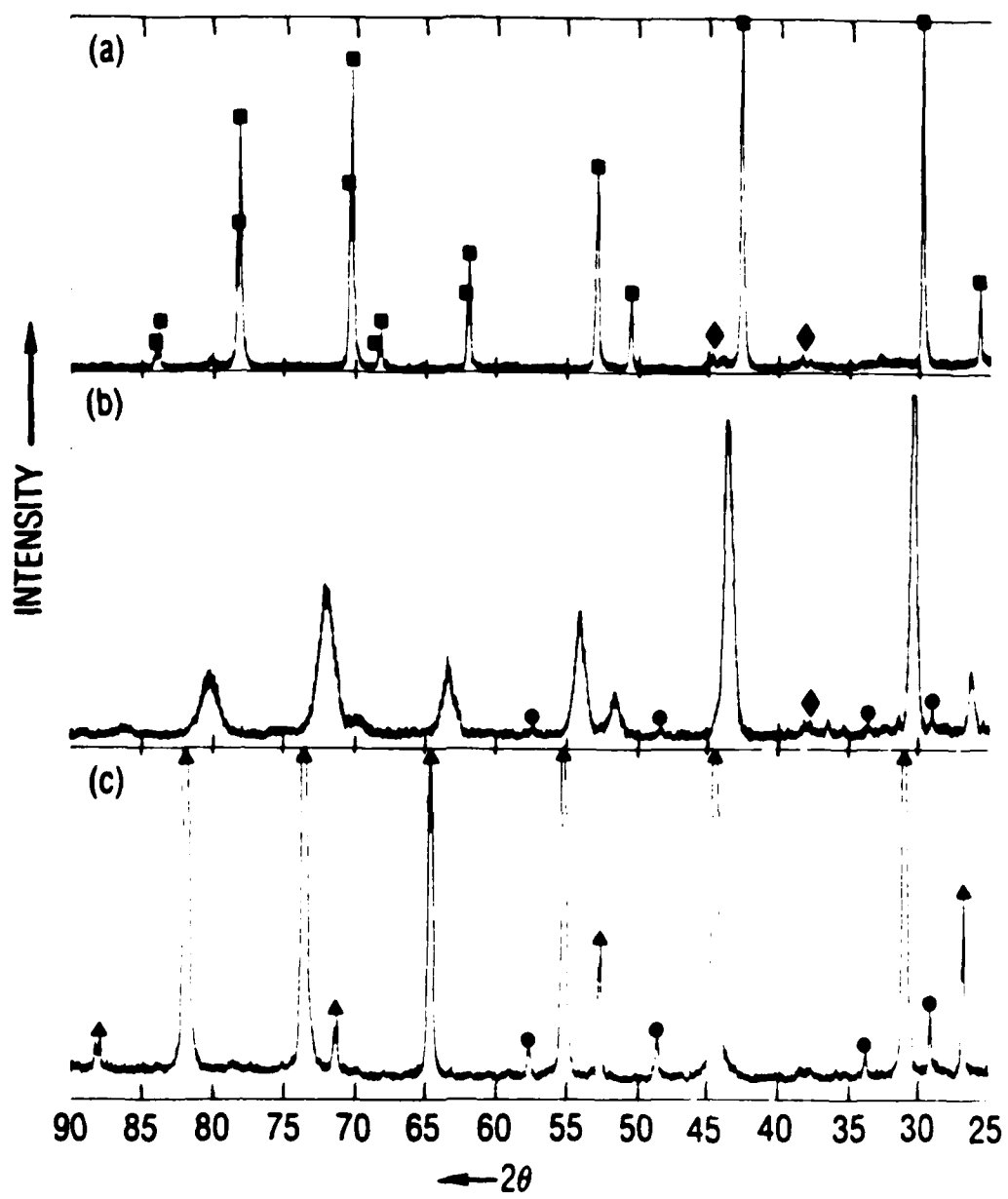


FIGURE 4-5. X-ray Diffractometer Charts of

- (a) NdAs#4
- (b) HoAs#5(Nd)
- (c) HoAs#2

NdAs ■ Al ♦ Ho₂O₃ • HoAs ▲

Table 4-5. Chemical Analysis of HoAs(Nd) Solid Solutions

Sample	Type Of Analysis	Results			
		zNd	zHo	zAs	zSi
HoAs#2(Nd)	EDXS	28	31	41	X
	EDXS	> 25	> 30	> 44	X
HoAs#3(Nd)	EDXS	31	38	31	X
	EDXS	31	33	36	X
HoAs#5(Nd)	EDXS	22	33	45	X
	EDXS	22	37	41	X
HoAs#6(Nd)	EDXS	0	52	45	3
	EDXS	5	53	< 42	1
	EDXS	0	55	44	1
HoAs#5(Nd)	ICP-AES	19.9%	37.9%	42.0%	.2%

X not determined

4.5 DETERMINATION OF LATTICE PARAMETER, a_0

In a cubic system such as the NaCl structure, the relation between "a", the lattice parameter, and the Miller indices of a plane (hkl) is given by

$$a = d \sqrt{h^2 + k^2 + l^2} \quad (1)$$

where d , the interplanar spacing, is calculated from Bragg's law,

$$n\lambda = 2d \sin\theta \quad (2)$$

Bragg's law must be satisfied if diffraction is to occur. λ is the wavelength of the incident x-rays, θ is the angle of incidence and n is an integral number of wavelengths. Because the error in $\sin\theta$ caused by a given error in θ decreases as θ approaches 90° , the error in d is also minimized as θ approaches 90° or as 2θ approaches 180° . The chief sources of error in θ in a Debye-Scherrer camera include film shrinkage, incorrect camera radius, off centering of the specimen and absorption in the specimen.

By loading the film in an unsymmetrical or Straumanis fashion, film shrinkage correction is already obtained without calibration concerns and the camera radius dimension need not be known. (22)

Furthermore, the fractional errors in d due to off centering and absorption of the specimen can be derived as being directly proportional to $\cos^2\theta$:

$$\frac{\Delta d}{d} = K \cos^2\theta \quad (3)$$

In addition, since

$$\frac{\Delta d}{d} = \frac{\Delta a}{a} = \frac{a - a_0}{a_0} \quad (4)$$

"a" can be described by

$$a = a_0 + a_0 K \cos^2\theta \quad (5)$$

where a_0 is the true value of lattice parameter. Thus, if "a" values are computed for each line on the diffraction pattern and plotted against $\cos^2\theta$, a straight line should result. The extrapolated value of "a" at $\cos^2\theta = 0$ will be the true lattice parameter constant, a_0 . This extrapolation is valid only when large values of θ are applied.

In this work, λ values of 1.540562 Å for $\text{CuK}\alpha_1$ and 1.544390 Å for $\text{CuK}\alpha_2$ were used to calculate the interplanar spacing, d . For most samples only diffraction lines corresponding to θ values greater than 60° (usually between 10 to 12 lines) were included for the determination of the lattice parameter.

4.5.1 Results Of Lattice Parameter Measurements

The lattice parameter (a_0) values calculated for the NdAs and HoAs compounds are listed in Table 4-6. Consistent values were found between different batches for each compound. NdAs and HoAs were found to have lattice parameters of 5.995 Å and 5.768 Å respectively. Even those samples that underwent TGA or DSC retained almost exactly the same a_0 value. Compared to the value reported in the x-ray diffraction card files, the synthesized NdAs has a larger a_0 value by .025 Å. However, compared to the findings of Aeby et al.⁽¹⁾ who reported a value of 5.994 Å and Taylor et al.⁽⁷⁾ where a_0 was determined to be 5.995 Å, the lattice parameter is in excellent agreement with previously existing compounds. The lattice parameter of the synthesized HoAs is comparable to that recorded in the card files. Lattice parameter values were also calculated for each phase in the (Ho,Nd)As compounds whenever feasible, and are listed in Table 4-7. At least five diffraction lines corresponding to $\theta > 53^\circ$ had to be present on the film for the calculation. Again, all the NdAs values and HoAs values in each (Ho,Nd)As synthesis remained nearly the same as the pure binary compounds. No expansion or contraction of the lattice was evident in these mixed compounds.

Table 4-6. Lattice Parameters of the NdAs and HoAs Compounds at Room Temperature

Sample	Calculated Lattice Parameter a_0 (Å)	Sample	Calculated Lattice Parameter a_0 (Å)
NdAs #1	5.995	HoAs #1	5.768
NdAs #2	5.995	HoAs #2	5.768
NdAs #3	5.995	HoAs #3	5.769
NdAs #4	5.994	HoAs #5	5.768
NdAs #5	5.995	HoAs #6	5.765
NdAs #3 after TGA	5.996	HoAs #7	5.768
		HoAs #1 after TGA	5.768
		HoAs #6 after DSC	5.768
Average value NdAs#	5.995 ± .001	Average value HoAs#	5.768 ± .001
NdAs card ^a	5.970	HoAs card ^b	5.771

^a X-ray diffraction card file (1937)

^b X-ray diffraction card file (1961)

Table 4-7. Lattice Parameters of the (Ho,Nd)As Compounds at Room Temperature

Sample	Calculated Lattice Parameter, a_0 (Å)	
	NdAs	HoAs
(Ho,Nd)As #1	5.996	5.769
(Ho,Nd)As #2	5.995	5.768
(Ho,Nd)As #4	5.995	--
(Ho,Nd)As #5	5.994	5.766
(Ho,Nd)As #7	5.995	--
(Ho,Nd)As #8	--	5.768

-- not determinable

Because the diffraction patterns of the HoAs(Nd) solid solutions consisted of broad lines on the x-ray film, precise a_0 lattice parameter measurements could not be determined. Estimates of the lattice constant were identified from the diffractometer patterns. Selecting only the peak value of the diffraction peak corresponding to the 620 lattice plane, the d spacing was determined using Bragg's law. (The 422 plane was selected for the HoAs#2(Nd) sample.) From this information, $a = d\sqrt{h^2 + k^2 + l^2}$ was calculated and is listed in Table 4-8.

This procedure of determining "a" from one diffraction peak was performed on the HoAs compounds also using the 620 lattice planes. An average "a" value of 5.76 Å resulted. 5.76 Å was accurate to within 0.01 Å of the a_0 value calculated using precise lattice measurement techniques. Thus, it may be assumed that the estimated "a" values for the HoAs(Nd) solid solutions are of comparable accuracy.

**Table 4-8. Lattice Parameters of the HoAs(Nd) Solid Solutions
at Room Temperature**

Sample	Estimated Lattice Parameters, a (Å)
HoAs#2(Nd)	5.89
HoAs#3(Nd)	5.94
HoAs#5(Nd)	5.85
HoAs#6(Nd)	5.76

CHAPTER 5. CHARACTERIZATION OF THE ARSENIDES OF NEODYMIUM AND HOLMIUM

5.1 NdAs COMPATIBILITY TESTS

Prior to attempting any high temperature heating, sintering, or pressing of the NdAs, a container material suitable for these processes needed to be considered. Tests with Pt, Mo, graphite and boron nitride coated graphite were conducted to ascertain the reactivity of NdAs with these proposed container materials.

Platinum foil, 2 mil thick, was fashioned into a cone with the pointed end folded upwards to prevent the contents from leaking. A small amount of NdAs powder was poured into the Pt cone which was placed in a quartz tube and subsequently evacuated and sealed. The same furnace arrangement used in previous compound syntheses was utilized here. The furnace heating rate was established at approximately 20°C/min up to 1000°C. The quartz tube was held at 1010°C for 1 hour. Molybdenum foil was tested in a similar manner as platinum.

By drilling a blind hole down a graphite rod, a small graphite crucible was constructed. The crucible was filled with NdAs, and a lid (also made of graphite) was designed to plug the open end. As before, this assembly was placed in an evacuated, sealed, quartz tube, heated rapidly to 1000°C in the furnace and held at that temperature for 1 hour. The same crucible was tested again but the NdAs sample was added after the graphite had been coated with a boron nitride and acetone slurry and allowed to dry.

5.1.1 Results of the NdAs Compatibility Tests

A summary of the compatibility of NdAs with various materials is provided in Table 5-1. Platinum foil clearly proved to be an unsatisfactory container material as the NdAs powder reacted to form several small holes through the bottom of the Pt cone. The small amount of rare earth compound was not recoverable and an x-ray diffraction analysis was not obtained.

On visual inspection, the molybdenum foil appeared as shiny as before the reaction and remained intact. X-ray analysis of the powder compound suggested that some reaction might have occurred as very weak lines of possibly $\text{Nd}_6\text{MoO}_{12}$ or Nd_2O_3 appeared.

Table 5-1. Results of Compatibility Tests with NdAs

Sample	Visual	X-ray	Deposit at Top of Tube	X-ray of Deposit
NdAs #1 and Pt	NdAs reacted with the Pt cone	Sample not removed	No	X
NdAs #2 and Mo	No apparent reaction between NdAs and Mo	NdAs, possible $\text{Nd}_6\text{MoO}_{12}$	No	X
NdAs #2 and graphite	No apparent reaction between NdAs and graphite	NdAs	No	X
NdAs #3 BN coated graphite	BN turned from white to gray	Nd_2O_3	Yes, fine grey layer	$\text{As}, \text{As}_2\text{O}_3$

Except for what appeared to be some crazing at the bottom of the quartz tube, the heat treatment did not affect the graphite/NdAs system. Visually, the graphite crucible appeared undamaged and x-ray analysis of the compound disclosed no lines other than those attributable to NdAs crystals. In the BN coated graphite/NdAs system, a shiny grey layer formed at the top of the quartz tube after heating. When the x-ray analysis was performed, the deposit was no longer shiny and it was determined to be arsenic and As_2O_3 . The material in the BN coated graphite container consisted of neodymium and boron. Both EDXS and IMMA analyses confirmed there was no detectable amount of arsenic. The x-ray diffraction pattern indicated the material in the BN coated graphite container was no longer NdAs but rather Nd_2O_3 . The formation of Nd_2O_3 may be explained by the fact that the commercial BN used contained B_2O_3 as a binder and this oxide may have reacted with the NdAs.

5.2 THERMOGRAVIMETRIC ANALYSIS (TGA)

This analysis entails measuring the weight of a sample while that sample is heated according to a predetermined temperature program. The heating rate used in this analysis was $4^{\circ}C/min$. The measurement was performed between room temperature and $1000^{\circ}C$ under a flowing argon atmosphere.

The standard platinum basket sample holder was substituted with a specially made molybdenum basket. This change reflected the results obtained from the compatibility tests which showed that Mo

would be a more suitable container material than Pt for the arsenides. A TGA was first conducted on an empty basket in order to calibrate it. Approximately 20 mg of powdered sample was then weighed into the basket for the analysis. The output was a graph showing residual weight and percent weight loss versus temperature.

5.2.1 Results of Thermogravimetric Analysis (TGA)

TGA was carried out on one of each of the NdAs, HoAs and HoAs(Nd) compounds. Results of these TGA analyses are presented in Figures 5-1 a, b, and c. The TGA calibration for the empty molybdenum basket indicated a normal, slight downward drift in the weight of the molybdenum basket from buoyancy effects. Then between 700 and 800°C the basket weight began to increase until it partially or fully returned to its original weight at 1000°C. Curve III of Figures 5-1 a, b, and c shows the TGA for the molybdenum baskets. Originally a grey-metallic color, the molybdenum basket appears to have tarnished, rendering it a dull, dark grey color. The molybdenum surface was probably being oxidized at these elevated temperatures with whatever residual oxygen there was in the high purity argon gas. Because the weight change amounted to only about 1/4 percent, it was decided that the molybdenum oxide surface could be tolerated for the TGA. Ideally, a TGA analysis performed under vacuum would provide more inert conditions for analysis.

In the NdAs #3 sample (Figure 5-1a), a significant weight loss began at about 375°C. The loss continued gradually to about 800°C at which point the weight dropped again but this time more

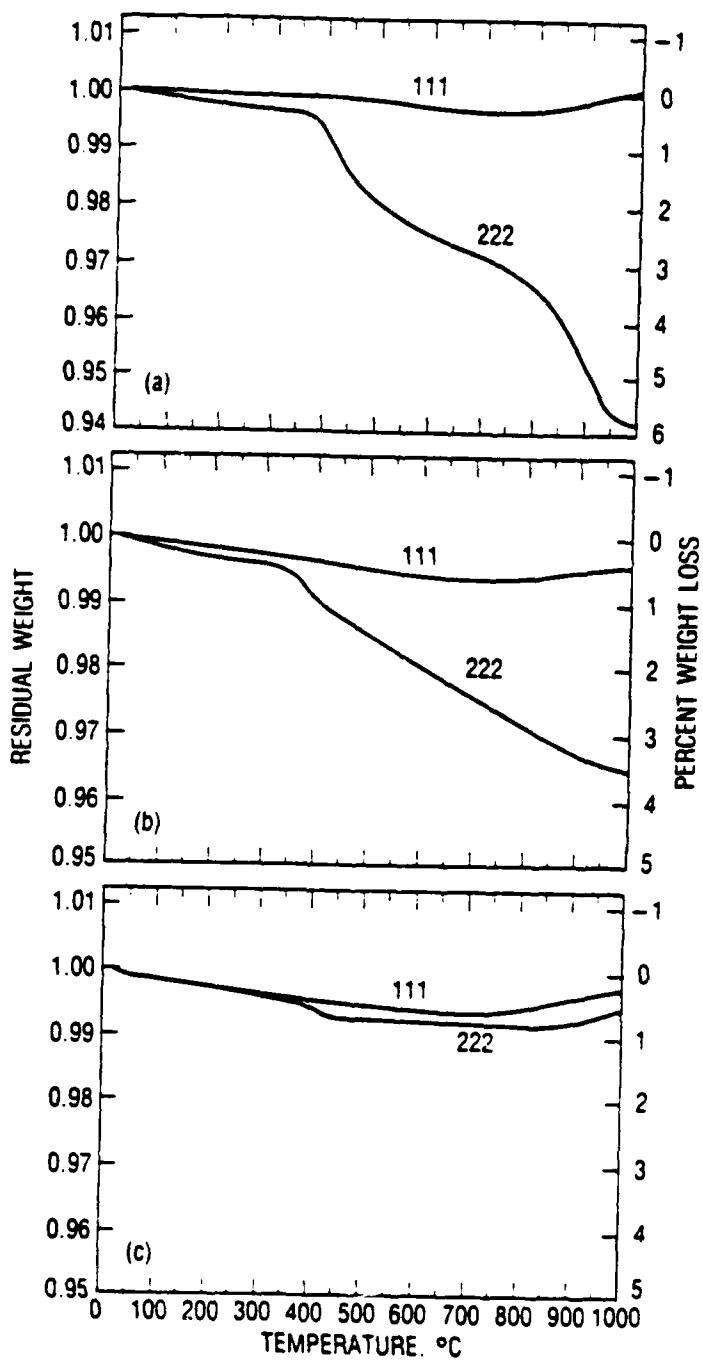


FIGURE 5-1. TGA in Argon

- (a) 111 Mo Basket, 222 NdAs#3
- (b) 111 Mo Basket, 222 HoAs#1
- (c) 111 Mo Basket, 222 HoAs#5(Nd)

rapidly until 1000°C. It appeared as if two separate events had taken place. The final weight loss was almost 6% of the initial weight. Upon inspection of the compound, the particles near the surface of the basket appeared to have turned light green in color while those below the surface remained grey-black. It was possible to obtain semi-quantitative chemical analysis on the two types of particles separately. EDXS analysis showed that the grey particles consisted of 63% Nd and 37% As and the green particles contained 83% Nd and 17% As. X-ray analysis of the grey particles still produced diffraction lines characteristic of NdAs with no noticeable shift in line positions and no appearance of free neodymium metal. However, it was evident that the thermal treatment leads to arsenic volatilization.

The TGA of HoAs #1 (Figure 5-1b) is somewhat similar to that of NdAs. HoAs #1 also lost weight (up to 3 1/2 % at 1000°C) but did so in one gradual descent from 375°C. The particles remained grey-black in color and post-TGA EDXS analysis yielded a concentration of 60% Ho and 40% As.

In contrast to the other arsenides, HoAs#5(Nd) appears stable as it showed very little weight loss. The TGA curve for this material (Figure 5-1c) closely followed the weight versus temperature curve of the empty molybdenum basket. Only over the range of 400 to 450°C was there a small observable drop (~ .3%) in weight. The dissimilar thermal behavior of HoAs#5(Nd) compared with NdAs and HoAs points to the different nature of the solid solutions from the binary arsenides.

5.3 DIFFERENTIAL SCANNING CALORIMETRY (DSC)

In DSC, the sample is subjected to a prescribed linear heating rate and the differential energy required to keep the sample conformed to this heating rate is measured. Thus, the endothermic or exothermic behavior of the sample can be monitored by observing the increase or decrease of heat input necessary to maintain a constant rate of temperature rise.

Weights of powdered samples analyzed varied between 2 and 23 mg. The samples were kept in an argon atmosphere during the experiment. Heating started at liquid nitrogen temperatures and proceeded up to 550° or 600°C at a rate of 10°C/min. The results are plotted on a graph depicting differential heat flow in milliwatts versus temperature. The specific heat of the sample can also be determined at various temperatures if its molecular weight is known.

5.3.1 Results of Differential Scanning Calorimetry (DSC)

The results of the Differential Scanning Calorimetry analyses of NdAs#4, HoAs#6 and HoAs#5(Nd) are presented in Figures 5-2 a, b and c. Although the compounds were examined from -160°C, no change in heat flow was observed in all compounds until at least 100°C.

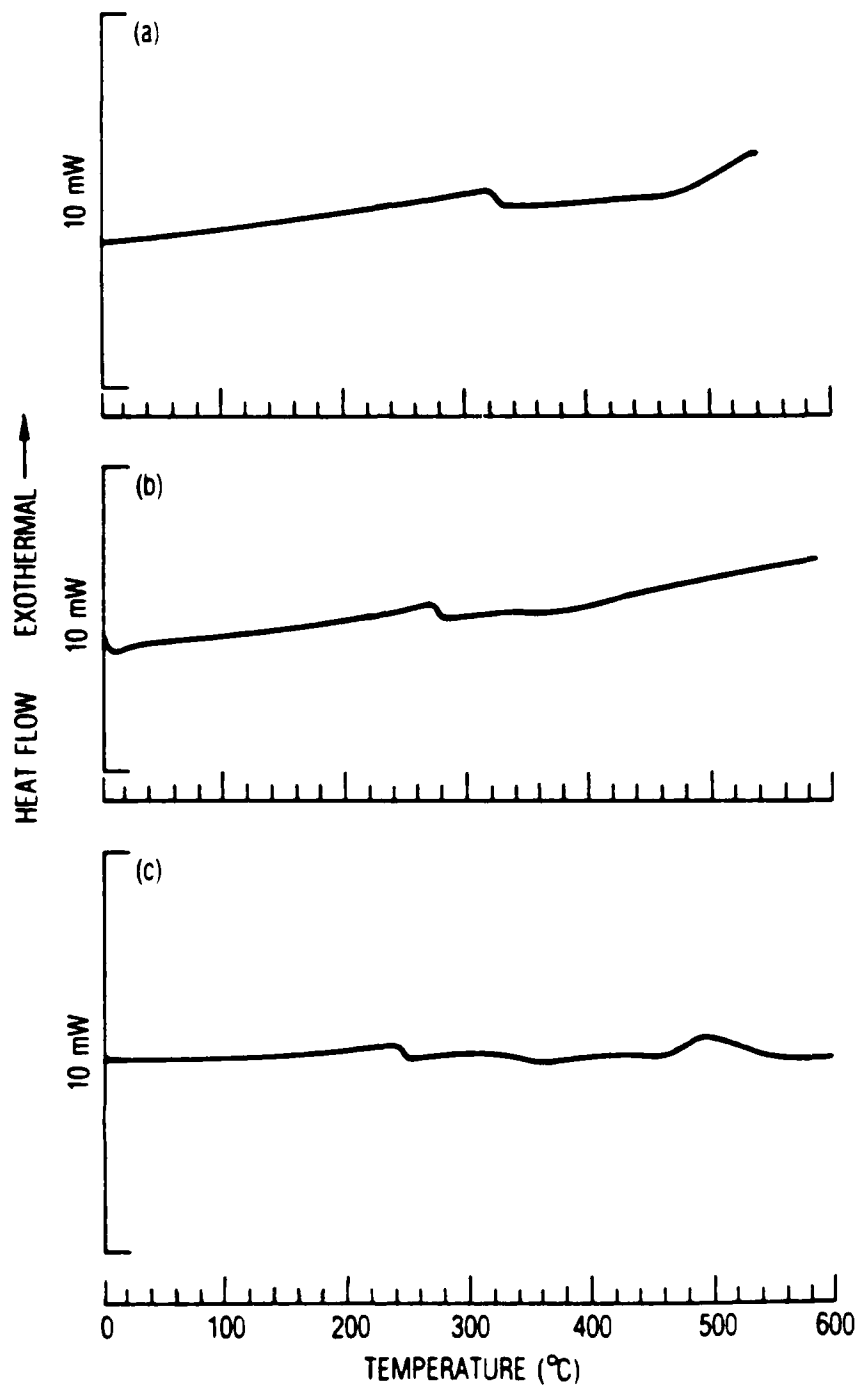


FIGURE 5-2. DSC in Argon

- (a) NdAs#4
- (b) HoAs#6
- (c) HoAs#5(Nd)

Five NdAs #4 samples were analyzed. Three of the samples ranging in weight from 2 to 18 mg each had one small exothermic peak between 250° and 350°C. In addition, there appeared to be a slight rise in heat flow near 500°C in these three samples. Figure 5-2a represents the DSC analysis of the 2 mg sampling which is typical of these three samplings. The fourth sample which weighed about 3 mg produced very little change in heat flow across all temperatures. The last sample (8 mg) was quite different with a very large exothermic rise (an order of magnitude larger than the small peaks). The exotherm emerged at 400°C and continued to the end of the experiment at 600°C.

Three separate DSC determinations of HoAs#6 were made using sample weights ranging from 16 to 21 mg. One small exotherm which peaked between 250°C to 300°C was revealed in each sample (Figure 5-2b). X-ray analysis of HoAs #6 after the DSC run showed one or two faint lines corresponding to H_2O_3 along with the HoAs pattern.

The thermal characteristics of five HoAs#5(Nd) samples were determined. Four samples (3 mg to 23 mg) exhibited definite exothermic behavior near 500°C. One of these four samples also included an exothermic peak at 240°C (see Figure 5-2c). The fifth sample showed very little change in heat flow across all temperatures.

In all the samples, the exothermic behavior may describe a decomposition phenomena.(23) The exothermic peaks generally occur between 250 - 500°C which encompasses the 300 - 400°C reaction temperature range of the binary arsenides. Coupled with the information from the TGA, x-ray analyses and the chemical composition results, it appears the DSC analyses also indicate the decomposing of the rare earth arsenides into an arsenic-poor alloy. In addition, the inconsistencies in the DSC results probably arise because of impurity effects and perhaps some oxidative degradation in the case of HoAs.

CHAPTER 6. DISCUSSION

6.1 PROPERTIES OF HoAs(Nd)

The syntheses of the HoAs(Nd) compounds have shown that substitutional solid solutions of various compositions of $\text{Ho}_x\text{Nd}_{1-x}\text{As}_{1-y}$ can be formed in the holmium-neodymium-arsenic system. The variation in lattice parameter with rare earth composition of the binary arsenides and the four HoAs(Nd) samples is depicted in Figure 6-1. Three of the four HoAs(Nd) samples lie on or near the dashed line which indicates Vegard's law. The law proposed by Vegard describes the relationship where the lattice spacing of solid solutions varies linearly in proportion to the atomic percent and size of the component atoms present. For this reason, Vegard's law will be observed only in solid solutions where the size factor of the components is the main influence on the lattice spacings.⁽²⁴⁾

In Figure 6-1, the lattice parameter value of HoAs#3(Nd) is markedly higher than what would be expected for its composition if Vegard's law were to apply. One possible explanation for this behavior is that there is a formation of an intermediate compound (also NaCl crystal structure) and the distinct increase in lattice parameter indicates the phase boundary. However, a more complete series of alloys would be necessary to confirm this. So far, there are no alloys which represent the expected two phase region that would connect the terminal solid solution with the intermediate phase.

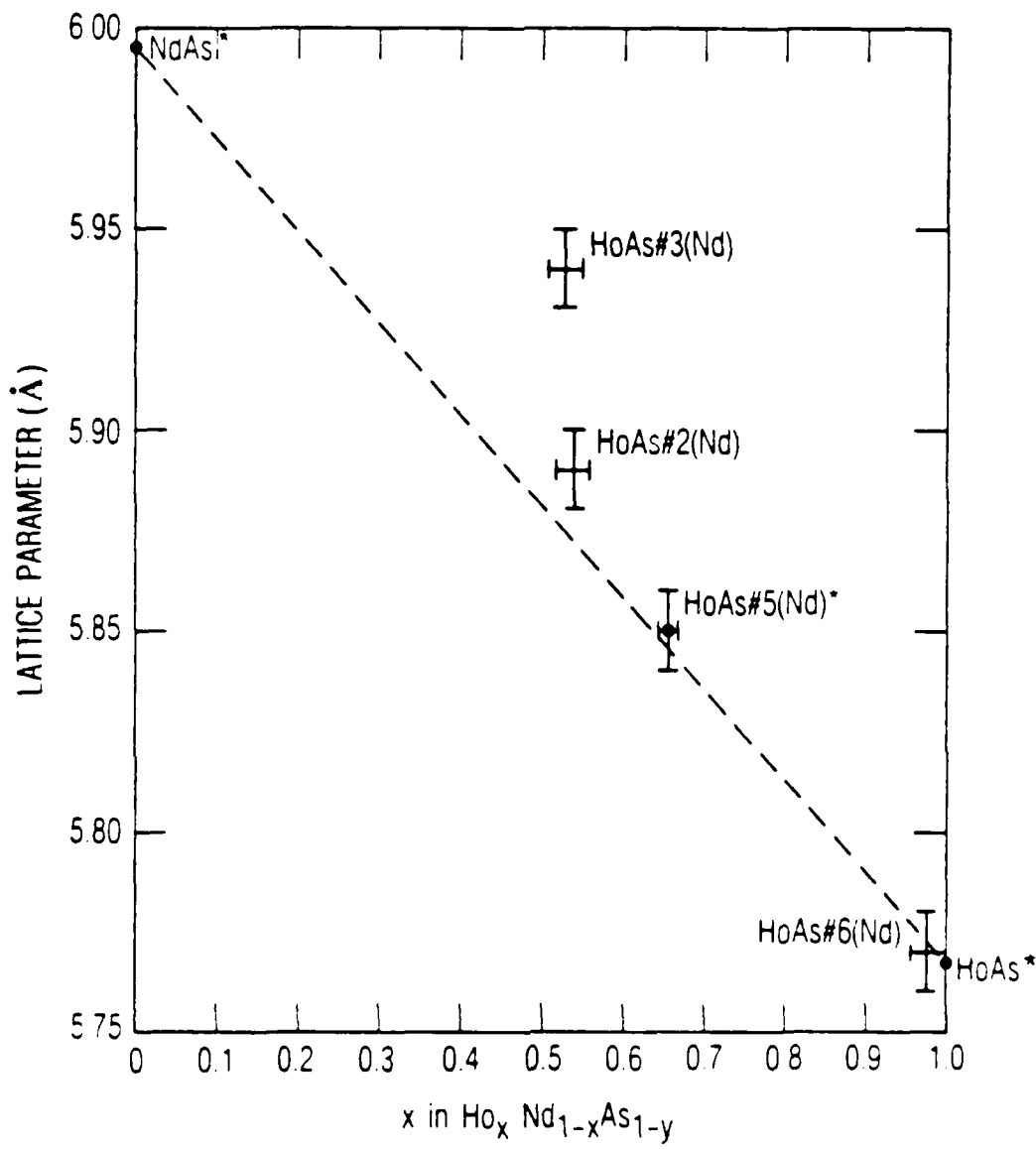


FIGURE 6-1. Lattice Parameter Versus Chemical Composition of $\text{Ho}_x \text{Nd}_{1-x} \text{As}_{1-y}$

Dashed Line Indicates Vegard's Law

*Chemical Composition Analyzed by ICP-AES
All others analyzed by EDXS

The synthesis of HoAs#6(Nd) led to a product of unexpected composition. Although HoAs#6(Nd) started with the same nominal HoAs to Nd ratio as HoAs#5(Nd), there was very little incorporation of Nd into the HoAs#6 structure. The difference between the two syntheses was the prolonged heat treatment of HoAs#6(Nd) at 1050°C. Instead of producing a further homogenized $Ho_xNd_{1-x}As$ phase, however, the 48 hour heat treatment produced constituent #1 comprised of mainly HoAs with some Ho_2O_3 and constituent #2, the products of reaction with the silica tube container.

It is believed that during the shorter reaction periods (12 hours and less), the Nd melt reacts with the HoAs, substituting with the Ho in the arsenide structure. Some of the holmium then reacts with the silica container wall, forming silicide and oxide products. The Nd melt reacts with the container as well. In the longer reaction, the continued heating allows greater exposure of the neodymium to the container material. As more Nd is consumed in this longer reaction with the silica, less is available for the $Ho_xNd_{1-x}As_{1-y}$ solid solution. Consequently, the solid solution becomes richer in holmium.

In both reaction sequences, it is obvious that the reaction with the quartz tube container is inevitable. An experimental test was performed to see what products would form upon heating holmium metal with crushed quartz powder using the same reaction conditions as with HoAs#5(Nd). The main product was Ho_2O_3 followed by $HoSi_2$ with possibly some $HoSi$. The Ho_2Si_3 form of silicide (which was found in the HoAs#5(Nd) reaction) was not detected by x-ray analysis. Data on

rare earth silicide heats of formation was not available. However, the relative ease of formation of the oxides can be seen for Ho_2O_3 , $\Delta H_{298}^0 = -449.5$ kcal/mol and Nd_2O_3 , $\Delta H_{298}^0 = -432.1$ kcal/mol. (25)

6.2 EFFECTS OF THERMAL ANALYSIS ON THE RARE EARTH ARSENIDES

One effect the thermal analyses had on HoAs#5(Nd) was the apparent homogenizing of the arsenide. This was evidenced by the appearance of less broad x-ray diffraction pattern lines. The line positions were the same as those determined before the TGA or DSC analysis. However, the line widths were sharper and narrower after the thermal treatment. Table 6-1 summarizes the effects of thermal analyses on the structure and composition of the rare earth arsenides.

In the binary arsenides, it was established that the lattice parameter was the same whether the arsenide had undergone thermal analyses or not. The chemical and x-ray analyses, however, showed that after the TGA, NdAs was more arsenic deficient than before. In fact, the arsenic content dropped from 47% to 37% of the total composition, yet the NdAs crystal structure still retained its original lattice parameter. This unusual behavior where variations in arsenic content can occur with no detectable change in lattice parameter was also observed in the work by Taylor et al. (7) with samarium arsenide and praseodymium arsenide. Taylor et al. also predicted that other rocksalt rare earth arsenides would behave in a similar manner but offered no explanation.

Table 6-1. Summary of Effects of Thermal Analyses on the Structure and Composition of the Rare Earth Arsenides

X-ray Diffraction Analysis	Lattice Parameter (Å)	EDXS ANALYSES CHEMICAL COMPOSITION (%)				
		Nd	Ho	As	Si	Other
HoAs#5(Nd)	Broad lines-Ho _x Nd _{1-x} As (Ho ₂ O ₃)	*19.9	37.9	42.0	.2	--
after TGA	Lines less broad-Ho _x Nd _{1-x} As no detectable shift in lines (Ho ₂ O ₃)			---		
after DSC	Lines less broad-Ho _x Nd _{1-x} As no detectable shift in lines (Ho ₂ O ₃)			---		
NdAs#3	NdAs	5.995	46	0	47	-
after TGA	NdAs	5.996	63	0	37	-
NdAs#4	NdAs	5.994	*50.8	0	49	.2
after DSC	NdAs	5.995		---		-
HoAs#1	HoAs, (Ho ₂ O ₃)	5.768	0	59	41	-
after TGA	HoAs, (Ho ₂ O ₃)	5.768	0	60	40	-
HoAs#6	HoAs	5.765	*0	58.5	41.4	.1
after DSC	HoAs, (Ho ₂ O ₃)	5.768		---		-

-Not determined

*Chemical analyses by ICP-AES

†Anomalous % of Ag

HoAs also incurred arsenic loss upon heating, but the loss was not as dramatic as in the case of NdAs. This may be because the HoAs was originally much more arsenic deficient. Again, no change in lattice parameter was observed after the thermal analyses.

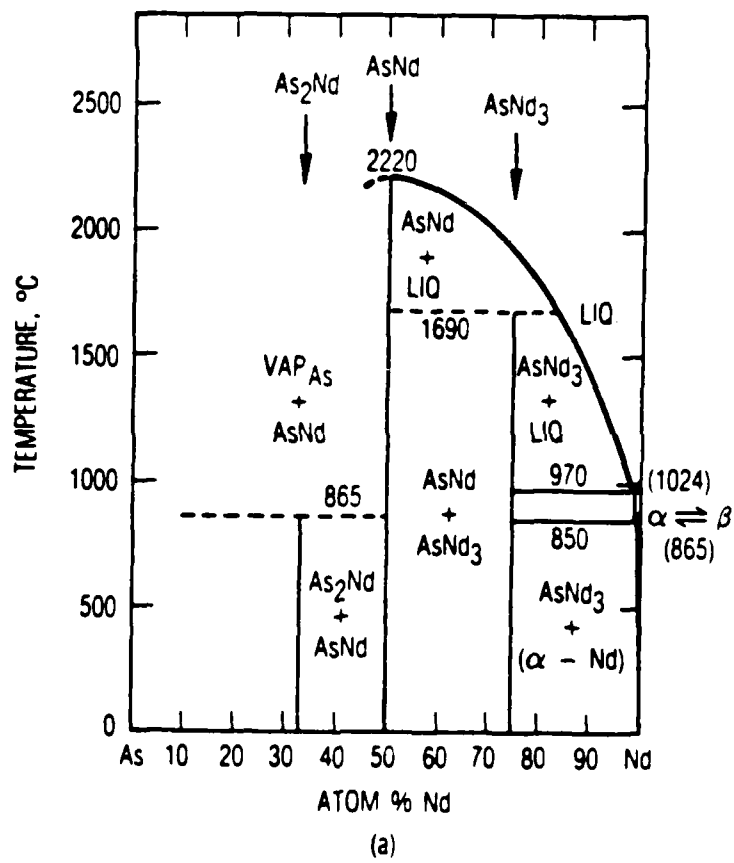
6.3 PROPERTIES OF NdAs and HoAs

Both the NdAs and HoAs products were synthesized using the solid-solid direct reaction procedure. Chemical analysis of the binary arsenides proved them to be arsenic deficient. This result is not surprising as others have reported preparing nonstoichiometric pnictides.(7,16,19,21) However, considering the chemical similarity of holmium and neodymium, the much greater departure from 1:1 stoichiometry of the HoAs compounds compared to the NdAs compounds was unexpected. In particular, the composition of NdAs#4 was determined to be $\text{Nd}_{1.0}\text{As}_{0.96}$ while that of HoAs#6 was $\text{Ho}_{1.0}\text{As}_{0.70}$.* Furthermore, in the HoAs syntheses, these were instances of impurity oxide formation while none was detected in the NdAs syntheses. Nevertheless, both pure rare earth metal reactants were handled in a similar manner and both HoAs and NdAs have nearly the same heat of formation values (see Table 2-4). Thus far, no explanation can be given for these observations.

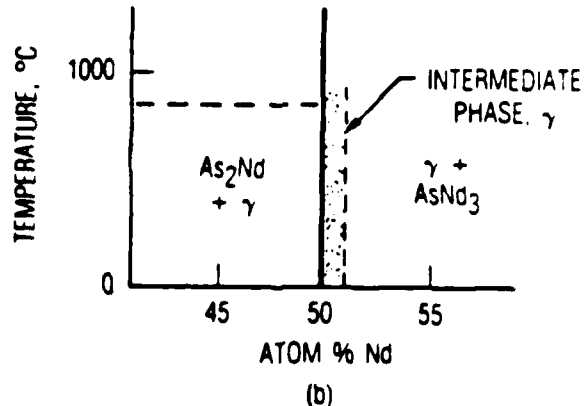
*Note that the compositions are based on the assumption of complete occupation of cation sites. No calculations were attempted to determine both cation and anion vacancies although previous work reported by Taylor et al.(7) has shown that in rare earth arsenides both lattices are deficient. Since the reported data on neodymium and holmium arsenides showed greater than 99% occupation of sites, the assumption was deemed reasonable.

It is interesting to note also that the lattice parameter determined for the HoAs synthesized in this study ($a_0 = 5.768 \pm .001$) is the same as that reported in the literature⁽⁷⁾ ($a_0 = 5.7684 \pm .002$, calculated formula = $\text{Ho}_{0.993}\text{As}_{0.947}$). But, the arsenic content is different by nearly 25 atomic percent. This is truly a large range of arsenic solubility over which a single lattice parameter value extends. No phase diagram data or other similar research on the alloys of the Ho-As system was available.

Kobzenko et al.⁽²⁶⁾ have constructed a Nd-As equilibrium diagram which is reproduced in Figure 6-2a. The arsenides with 50 atomic percent and less arsenic have been made by fusion in an electric arc furnace. NdAs is shown as a compound with a single composition of 50% Nd and 50% As. However, in this work, it has been determined that the arsenide can exist with an arsenic concentration of less than 50%; in particular, 49% As and 51% Nd for NdAs#4. Thus, instead of a single composition NdAs compound, an intermediate phase, γ , ranging from 50% to 49% (or possibly less -- recall the NdAs product after TGA) arsenic would better describe the solid solutions which can be formed (Figure 6-2b). No evidence of an Nd_3As compound formation was found in this research. Similar to the Nd-As system, the Ho-As system may include an intermediate phase that represents the solid solution with a composition of at least 50% to 41% arsenic.



(a)



(b)

FIGURE 6-2a. Equilibrium Diagram of the As-Nd System⁽²⁶⁾

6-2b. Intermediate Phase Formation in As-Nd System
Near 50 atomic % Nd

CHAPTER 7. CONCLUSIONS

Solid solutions of a new material, $Ho_xNd_{1-x}As_{1-y}$, can be prepared by reacting HoAs with Nd melt in evacuated, sealed quartz tube containers. By monitoring the reaction parameters, different compositions of the alloy can be formed. In general, the lattice parameter of these arsenides varies with the Nd to Ho content in accordance with Vegard's law. Reaction of the rare earth metal with the silica container cannot be ignored in these syntheses.

The binary arsenides, NdAs and HoAs, can be prepared using the solid-solid direct reaction technique. The compounds formed are arsenic deficient, particularly in the case of holmium arsenide ($Ho_1As_{.70}$). The composition of NdAs is $Nd_1As_{.96}$. The lattice parameter for these arsenides (HoAs:5.768 Å, NdAs:5.995 Å) match those in the literature for compounds with compositions nearer the 1:1 stoichiometry. It has been confirmed that a range of arsenic solubility exists in HoAs and NdAs where no change in lattice parameter is observed. The $Ho_xNd_{1-x}As_{1-y}$ alloy cannot be synthesized by this direct reaction method. When Ho, Nd and As elements are reacted together, the separate binary arsenides will form.

The binary arsenides decompose upon heating to become further arsenic deficient alloys. The observable weight change during thermal analysis is due to the arsenic volatilization. The $Ho_xNd_{1-x}As_{1-y}$ solid solution is more thermally stable as very little weight loss was recorded during the thermal analysis. In fact, the thermal treatment appears to reduce the chemical inhomogeneities in the arsenide.

CHAPTER 8. FURTHER SUGGESTIONS FOR STUDY

The ultimate goal of this research is to identify regenerator materials for cryogenic refrigerators. Further work towards this goal would therefore be to prepare the rare earth arsenide alloys for heat capacity measurements. This work would entail forming a series of bulk specimens at definite composition intervals from $x=0$ to 1 in $\text{Ho}_x\text{Nd}_{1-x}\text{As}$. Specimens of definite compositions may be easier to form if another preparation method for $\text{Ho}_x\text{Nd}_{1-x}\text{As}$ were established where a fixed Ho to Nd concentration is predetermined before the reaction is started. One such method may be to first synthesize various solid solutions of Ho-Nd alloys of known compositions. Then these rare earth alloys may be reacted with arsenic to form the arsenide.

Measuring heat capacity per unit volume of $\text{Ho}_x\text{Nd}_{1-x}\text{As}$ at cryogenic temperatures would reveal if these materials are suitable absorbers of heat at low temperatures and possible candidates for use in cryogenic refrigerators.

CeAs may be another rare earth arsenide that could be alloyed with NdAs to produce a compound with a large heat capacity between 7 and 11 K. Like NdAs, CeAs is also a Type I AFM (magnetization $\uparrow\downarrow[100]$); its T_N is about 7 K. The ionic radii of cerium and neodymium are very close as the elements are found next to each other in the periodic table. However, CeAs is not as dense as NdAs, and this is important for calculating heat capacity per unit volume. The heat capacity of CeAs has already been measured at its magnetic transition temperature and is approximately $0.3\text{J/K} \cdot \text{cm}^3$.⁽¹⁸⁾

Although this value is not very large, the fact that the heat capacity is known already gives us more information as to what the heat capacity versus temperature curve may look like for cerium neodymium arsenide.

REFERENCES

1. A. Aeby, F. Hulliger and B. Natterer, "Specific Heat and Schottky Anomalies of CeP, CeAs, NdP, and NdAs," Solid State Communications, 3(1973), pp. 1365-1368.
2. Douglas B. Mann, "The Thermodynamic Properties of Helium from 3 to 300°K between 0.5 and 100 Atmospheres," National Bureau of Standards Technical Note 154, January 1962.
3. "Specific Heat - Metallic Elements and Alloys," The TPRC Data Series Volume 4, ed. Y. S. Touloukian (IFI/Plenum, 1978), pp. 115-116.
4. K. H. J. Buschow, J. F. Olijhoek, and A. R. Miedema, "Extremely Large Heat Capacities Between 4 and 10K," Cryogenics, May 1975, pp. 261-264.
5. F. Hulliger, "Rare Earth Pnictides," Handbook on the Physics and Chemistry of Rare Earths, ed. K. A. Gschneidner, Jr. and L. Eyring (North-Holland Publishing Company, 1979), pp. 153-193.
6. A. Iandelli and E. Botti, Atti Accad. Lincei VI, 2G(1937), p. 233.
7. J. B. Taylor, L. D. Calvert, J. G. Despault, E. J. Gabe, and J. J. Murray, "The Rare-Earth Arsenides: Non-Stoichiometry in the Rocksalt Phases," Journal of Less-Common Metals, 37(1974), pp. 217-232.
8. A. Iandelli, Z. Anorg. Chem., 288(1955), p. 81.

9. A. Iandelli, "Cell Dimensions and Magnetical Susceptibilities of the MX Compounds of Rare Earths with P, As, Sb, Bi, S, Se, Te," Rare Earth Research, ed. O. Kleber (Publishing Company, 1961), pp. 135-141.
10. L. H. Brixner, "Structure and Electrical Properties of Some New Rare Earth Arsenides, Antimonides and Tellurides," J. Inorg. and Nuclear Chem., 16(1960), pp. 199-201.
11. D. H. Templeton and C. H. Dauben, J. Am. Chem. Soc., 76(1954), p. 5237.
12. S.E.R. Hiscocks and J. B. Mullin, "An Investigation of the Preparation and Properties of Some IIIa-VIb Compounds," Journal of Materials Science, 4(1969), pp. 962-973.
13. R. Hanks and M. M. Faktor, "Quantitative Application of Dynamic Differential Calorimetry, Part 2," Trans. Faraday Soc., 63(1967), pp. 1130-1135.
14. G. Busch and O. Vogt, "Magnetic Properties of Ordering Heavy Rare-Earth Arsenides," Physics Letters, 15, 4(April, 1965), pp. 301-303.
15. T. Tsuchida, Y. Nakamura and T. Kaneko, "Magnetic Properties of Neodymium Compounds with Va Elements," Journal of the Physical Society of Japan, 26, No. 2(February, 1969), pp. 284-286.
16. J. F. Miller, et al., "Study of Semiconducting Properties of Selected Rare-Earth Metals and Compounds," U. S. Department of Commerce, Technical Report No. AL TDR 64-239, 12 October 1964.

17. F. J. Ried, L. K. Matson, J. F. Miller, and R. C. Himes, "Electrical Properties of Selected Rare Earth Compounds and Alloys," Journal of the Electrochemical Society, 111, No. 8 (August, 1964), pp. 943-950.
18. F. Hulliger and H. R. Ott, "Low Temperature Thermal and Magnetic Properties of CeP and CeAs," Z. Physik B, 29(1978), pp. 47-59.
19. G. Busch, "Magnetic Properties of Rare-Earth Compounds," Journal of Applied Physics, 38, 3(March, 1967), pp. 1386-1394.
20. G. Busch, P. Schwob and O. Vogt, "Magnetic Anisotropies in HoP, HoAs, and HoSb," Physics Letters, 23, 11(December, 1966), pp. 936-939.
21. F. Hulliger, "Magnetic Properties of the Rare Earth Pnictides," Journal of Magnetism and Magnetic Materials, 8(1978), pp. 183-205.
22. B. D. Cullity, Elements of X-ray Diffraction, 2nd ed. (Addison-Wesley Publishing Company, 1978), pp. 352-355.
23. W. W. Wendlandt, Thermal Methods of Analysis, (Wiley, 1974), p. 230.
24. W. B. Pearson, Handbook of Lattice Spacings and Structures of Metals, (Pergamon Press, 1958), p. 23.
25. Handbook of Chemistry and Physics, 64th Edition, ed. Robert C. Weast (CRC Press, Inc., 1983), pp. D-69, D-76.
26. G. F. Kobzenko, V. B. Chernogorenko, S. N. L'vov, M. I. Lesnaya, and K. A. Lynchak, "Equilibrium Diagram and Properties of Alloys of the As-Nd System," Russian Journal of Inorganic Chemistry, 20, 8 (August 1975), pp. 1205-1208.

LABORATORY OPERATIONS

The Aerospace Corporation functions as an "architect-engineer" for national security projects, specializing in advanced military space systems. Providing research support, the corporation's Laboratory Operations conducts experimental and theoretical investigations that focus on the application of scientific and technical advances to such systems. Vital to the success of these investigations is the technical staff's wide-ranging expertise and its ability to stay current with new developments. This expertise is enhanced by a research program aimed at dealing with the many problems associated with rapidly evolving space systems. Contributing their capabilities to the research effort are these individual laboratories:

Aerophysics Laboratory: Launch vehicle and reentry fluid mechanics, heat transfer and flight dynamics; chemical and electric propulsion, propellant chemistry, chemical dynamics, environmental chemistry, trace detection; spacecraft structural mechanics, contamination, thermal and structural control; high temperature thermomechanics, gas kinetics and radiation; cw and pulsed chemical and excimer laser development including chemical kinetics, spectroscopy, optical resonators, beam control, atmospheric propagation, laser effects and countermeasures.

Chemistry and Physics Laboratory: Atmospheric chemical reactions, atmospheric optics, light scattering, state-specific chemical reactions and radiative signatures of missile plumes, sensor out-of-field-of-view rejection, applied laser spectroscopy, laser chemistry, laser optoelectronics, solar cell physics, battery electrochemistry, space vacuum and radiation effects on materials, lubrication and surface phenomena, thermionic emission, photo-sensitive materials and detectors, atomic frequency standards, and environmental chemistry.

Computer Science Laboratory: Program verification, program translation, performance-sensitive system design, distributed architectures for spaceborne computers, fault-tolerant computer systems, artificial intelligence, microelectronics applications, communication protocols, and computer security.

Electronics Research Laboratory: Microelectronics, solid-state device physics, compound semiconductors, radiation hardening; electro-optics, quantum electronics, solid-state lasers, optical propagation and communications; microwave semiconductor devices, microwave/millimeter wave measurements, diagnostics and radiometry, microwave/millimeter wave thermionic devices; atomic time and frequency standards; antennas, rf systems, electromagnetic propagation phenomena, space communication systems.

Materials Sciences Laboratory: Development of new materials: metals, alloys, ceramics, polymers and their composites, and new forms of carbon; non-destructive evaluation, component failure analysis and reliability; fracture mechanics and stress corrosion; analysis and evaluation of materials at cryogenic and elevated temperatures as well as in space and enemy-induced environments.

Space Sciences Laboratory: Magnetospheric, auroral and cosmic ray physics, wave-particle interactions, magnetospheric plasma waves; atmospheric and ionospheric physics, density and composition of the upper atmosphere, remote sensing using atmospheric radiation; solar physics, infrared astronomy, infrared signature analysis; effects of solar activity, magnetic storms and nuclear explosions on the earth's atmosphere, ionosphere and magnetosphere; effects of electromagnetic and particulate radiations on space systems; space instrumentation.

END
DATE
FILMED
JAN
1988